RUHR-UNIVERSITÄT BOCHUM

Commissioning of an acoustic levitator

BACHELORTHESIS

Submitted by Anh Le Nguyen Duc

Mat.-Nr. 1080 1820 5620

Study subject Mechanical Engeneering

Submission date 28.02.2022

1st Supervisor Prof. Dr.-Ing. Andreas Kilzer

2nd Supervisor Prof. Dr.-Ing. Eckhard Weidner

Advisors Dipl.-Ing. Nils Mölders, M.Sc. Joline Hansen

Anh Le Nguyen Duc Commisioning of an acoustic levitator

Ruhr-Universität Bochum
Fakultät Maschinenbau
Lehrstuhl für Verfahrenstechnische Transportprozesse
Universitätsstraße 150
44780 Bochum

PREFACE

This bachelor thesis entitled “Commissioning of an acoustic levitator” is the confidential information of the research at the Ruhr University Bochum and the Fraunhofer Institute for Environmental, Safety and Energy Technology UMSICHT, Oberhausen.

This thesis would be only seen from the first and second supervisors and the eligible members of the committee. Any reproduction and publication or dissemination of the content of this thesis are not allowed under any circumstances.

This thesis might only be made available with the permission of the author, the university, and the company.

ABSTRACT

This thesis is written as a requirement of the “Mechanical Engineering” Bachelor program at Vietnamese-German University. It reports the content of my working progress during the last exchange semester of the program at RUHR University, Bochum and Fraunhofer UMSICHT.

Liquid thermophysical characteristics are critical in a variety of scientific research and industrial applications for exact knowledge of these qualities is required for design and a better understanding of technological procedures. Therefore, there is a need to investigate these properties. Determination of density, interfacial tension and viscosity under ambient pressure has available through several methods. However, to investigate these properties, previous methods require contact with sample, which consumes time or requires a certain amount of experimental substance. Additionally, data for these properties under high pressure is lacking. A method can be applied to provide contactless investigation of liquid drop under pressure is acoustic levitation. The aim is to commission an acoustic levitator to measure density, interfacial tension, and viscosity of liquids. First, the basic principle of acoustic levitation needed to understand the setup is explained. Then, recent developments of properties measurement using acoustic levitation is review. Next, the high-pressure acoustic levitator plant and its function is described. The limitations and restrictions of the setup is pointed out. Afterwards, methods and procedures for density, interfacial tension and viscosity are presented. Finally, the measurement of these properties is conducted, and the results are presented and discussed.

ACKNOWLEDGEMENTS

This thesis would be not possible without the guidance and assistance of several individuals who contribute their valuable supports for the implementation and completion of this work.

First and foremost, my sincere gratitude to Nils Mölders at Fraunhofer UMSICHT who offered precious support and encouragement throughout the course of work.

To Joline Hansen at Ruhr University Bochum, without her continuous guidance during the work at the university and insightful feedback, this thesis would not have materialized. I would especially express my gratitude to her for guiding me through the hard time of the work.

Then, I would like to express my deepest appreciation to my supervisor Prof. apl. Dr.-Ing. Andreas Kilzer for without him the thesis would not be possible

I would like to express my thanks to Damian Hintemann for the valuable support at the technical room and laboratory.

Thanks also go to all my colleagues at the Fraunhofer institute UMSICHT, who have accepted me as a part of the team and for their technical support.

I would also like to thank my friend, Bao, for supports and conducting together with me the tight-planned experiments in the high-pressure plant.

Last, but not certainly the least, I am deeply grateful to my parents who always have encouraged me throughout my studies.

TABLE OF CONTENTS

PREFACE I

ABSTRACT II

ACKNOWLEDGEMENTS III

TABLE OF CONTENTS IV

LIST OF FIGURES V

LIST OF TABLES VI

NOCLAMENTURE VII

1. INTRODUCTION 1

2. STATE OF THE ART 3

2.1. ACOUSTIC LEVITATION 3

2.2. PROPERTIES MEASUREMENT WITH ACOUSTIC LEVITATION 6

2.3. IMAGE ANALYSIS 7

3. ACOUSTIC LEVITATOR SETUP 13

3.1. EXPERIMENTAL SET UP 13

3.2. FUNCTION 15

3.3. LIMITATION AND RESTRICTIONS 20

4. COMMISSIONING AND EXPERIMENTS 22

4.1. MEASUREMENT OF DENSITY 22

4.1.1. METHODS 22

4.1.2. PROCEDURES 24

4.2. MEASUREMENT OF VISCOSITY AND INTERFACIAL TENSION 24

4.2.1. METHODS 28

4.2.2. PROCEDURES 30

4.3. RESULTS AND DISSCUSSION 31

4.3.1. DENSITY 31

4.3.2. INTEFACIAL TENSION AND VISCOSITY 33

5. CONCLUSION 38

REFERENCES 39

APPENDIX 42

LIST OF FIGURES

Figure 2.1 A Standing Ultrasonic wave [1] 4
Figure 2.2 Acoustic forces acting on a liquid drop [14] 5
Figure 2.3: Image of precision ruby sphere 8
Figure 2.4: Contour of a drop 9
Figure 2.5: Tilted drop with shifted (x, y) and rotated coordinate system (X, Y) 10
Figure 2.6: Volume determination [2] 11
Figure 3.1 Ultrasonic sonotrode [1] 13
Figure 3.2 Scheme of the high-pressure acoustic levitation system [2] 14
Figure 3.3: Realistic view of the high-pressure acoustic levitator setup 15
Figure 3.4: Detailed view of the reflector housing and the capillary located inside 17
Figure 3.5: High-pressure view cell with high-speed camera 18
Figure 3.6: Front of the viewcell and the lower part of the reflector housing 19
Figure 4.1: Aspect ratio against levitation voltage [2] 22
Figure 4.2: Displacement from pressure node versus levitation voltage [2] 23
Figure 4.3 Forces acting on a molecule in the bulk phase and at a surface. [35] 25
Figure 4.4: Relation between surface tension and surface age [2] 26
Figure 4.5: Couette flow of a fluid between two parallel plates. [2] 26
Figure 4.6: Amplitude modulation of the high frequency carrier wave [2] 29

LIST OF TABLES

Table 4.1: Results of density determination using acoustic levitation *32*

Table 4.2: Interfacial tension and viscosity measured with acoustic levitation at different time after drop injection *34*

Table 4.3: Results of image analysis *35*

Table 4.4: Results of interfacial tension determination using acoustic levitation *36*

Table 4.5: Results of viscosity determination using acoustic levitation *36*

NOCLAMENTURE

Latin Symbols

d	distance between transducer and reflector	m
$\hat{p}$	sound pressure	Pa
$\hat{v}$	sound velocity	$\frac{m}{s}$
F_z	axial acoustic positioning force	N
F_R	radial acoustic positioning force	N
F_{ax}	axial acoustic positioning force	N
g_0	gravitational acceleration	$\frac{m}{s^2}$
f	frequency	Hz
k_0	wave number	$\frac{1}{m}$
V_s	volume of spherical sample	m^3
d_s	diameter of spherical sample	m
Δz	distance between drop's centre and pressure node	m
c_0	speed of sound inside the gas medium	$\frac{m}{s}$
m_i	coordinates of drop center	$pixels$
x	x-coordinate of drop contour	$pixels$
y	y-coordinate of drop contour	$pixels$
X	x-coordinate rotated of drop contour	$pixels$
Y	y-coordinate rotated of drop contour	$pixels$
V	volume	m^3
r	radius	m
h	height of one pixel	m
U	levitation voltage	V_{pp}
G	Gibb's energy	J
A	area	m^2
p	pressure	MPa
T	temperature	K

F	Force	N
V_x	velocity	$\frac{m}{s}$
f_M	low frequency signal	Hz
f_c	high frequency signal	kHz
U_0	initial amplitude	V_{pp}
$U(t)$	carrier signal amplitude	V_{pp}
t	time	s
M	depth of amplitude modulation	$-$
l	mode of oscillation	$-$
R	Radius of the volume equal sphere	m
Oh	Ohnesorge number	$-$

Greek Symbols

λ_0	wavelength	m
ρ	density	$\frac{kg}{m^3}$
π	pi	$-$
α	rotation angle	°
σ	surface/interfacial tension	$\frac{N}{m}$
$\dot{\gamma}$	shear rate	$\frac{1}{s}$
η	Dynamic viscosity	Pas
τ	damping constant	$\frac{1}{s}$
τ_S	shear stress	Pa

1. INTRODUCTION

Physical properties of liquid have always been an interesting subject for scientific research and industrial application. Previously, to investigate a drop of an unknow liquid, a sample drop is produced precisely using a capillary. Thus, the sample must come into contact with the capillary, and results in a continuous heat and mass transfer between the pendant drop and the sample liquid in the capillary [1]. Due to this, a method that allows investigation of liquid drop without wall contact is needed. One prospect to examine liquids contactless is utilizing a levitation method. Levitation has been used for many years to manipulate materials within air and liquid environments without physical interaction with a surface. It aims to create a microgravity environment to study the materials which are levitated. There are many forms of levitation including acoustic, magnetic, electrostatic, optical, and aerodynamic principles [2, 3].

To levitate diamagnetic materials, magnetic levitation requires the sample to be either ferromagnetic or the magnetic fields to be among the greatest created on Earth [4]. To overcome gravity, electrostatic levitation employs an electric field to lift the sample, which demands a sample that can and must be charged [5]. Optical levitation, which is generated by firing a concentrated laser beam at the sample and utilizing the transfer of momentum from the photons to the sample surface, has only been performed for very tiny and lightweight particles. The particle's refractive index must be greater than the medium's for this approach to work. As a result, this method can only be used in a small number of circumstances [6]. Finally, aerodynamic levitation is done by suspending the material under examination with a high-pressure gas jet, however this creates tremendous agitation and may alter the investigating sample [7]. In contrast to the aforementioned approaches, acoustic levitation is a superior presentation method in a wide range of applications since the variety of materials that may be levitated is significantly wider because no sample attributes are required. The single axis acoustic levitation system generates a succession of positions in which the circumstances are ideal to entrap particles or sample droplets using an emitter and reflector that emits frequencies above those audible by the ordinary human [3].

Acoustic levitation was first devised as a way to perform microgravity research for space applications on Earth [8]. From then, mid-air acoustic levitation has become a powerful tool

for suspending and manipulating millimetric objects. Acoustic levitation can be also used in conjunction with noncontact measuring devices, allowing contactless characterization and analysis of levitating samples [9].

Time consuming measurement methods for binary systems lead to the lack of literature values for density, viscosity, and interfacial tension of liquids under high pressure. With the help of acoustic levitation, an efficient and contactless, method that does not require special properties of samples has been developed to measure these properties. The aim of this work is the commissioning of a high-pressured acoustic levitator and investigation of the setup's limitations. It considers the measurement of density, interfacial tension, and viscosity of liquids inside a saturated CO_2 atmosphere applying acoustic levitation.

In this thesis, the basic principle as well as the state of the art regarding measurements with acoustic levitation is explained to understand the apparatus and its purpose (chapter 2). Then, the setup of the high-pressure acoustic levitator plant and functions of the components are described thoroughly (chapter 3). Furthermore, the measurement techniques are examined under high pressure. To determine density, the voltage needed to levitate the desired liquids is compared with a reference material. For determination of interfacial tension and viscosity, a method is devised using drop shape oscillations and a Matlab© image analysis (chapter 2 and 4). Finally, the results will be compared to existing literature data. The limitations and restrictions of the methods will be discussed (chapter 4).

2. STATE OF THE ART

The purpose of this thesis is to commission an acoustic levitator. Therefore, in this section, the basic concept of single axis acoustic levitation is introduced to provide basic knowledge on the subject. Next, the state of art of physical properties measurement using acoustic levitation is reviewed. Finally, a Matlab© code used for the determination of physical properties is presented.

2.1. ACOUSTIC LEVITATION

Acoustic levitation indicates the suspension of miniature liquid or solid particles by utilizing acoustic radiation forces from ultrasonic waves [9, 10]. The sound waves, generated by a piezoelectric transducer, travel until they meet a reflector, at which they are reflected. The reflector is set up directly across from the transducer on the same axis as shown in Figure 2.1. Both are curved to improve the stability of the levitation. Hence, interference of the emitted and reflected waves occurs. Here, a stationary sound field is brought about if and only if resonance condition is satisfied. Resonance happens when the distance d (in m) between the transducer and the reflector is equals to an integer multiple of half the emitted wavelength λ_0 (in m) [11, 12].

$$d = n \cdot \frac{\lambda_0}{2} (n = 1,2, \dots, n) \tag{2.1}$$

A standing sound waves is characterized by a sequence of low energy density areas (pressure nodes) and high energy density areas (antinodes). The sound pressure and sound velocity amplitudes are denoted as $\hat{p}_{max}$ and $\hat{v}_{max}$, respectively. While the sound pressure and velocity nodes are $\hat{p}_z = 0$, and $\hat{v}_z = 0$. Small samples of liquid and solid can be placed just below the sound pressure nodes. Below the drop, the mean sound pressure is higher than above. The resulting pressure differential balances the sample's weight and allows the drop to be placed without supporting it [11–13]. Another factor in the positioning of the drop in mid-air is the sound velocity. It is illustrated by the speed of sound-transmitting particles traveling back and forth in the acoustic field and prevents lateral migration of the levitated sample. The sound velocity reaches its maximum at the places of the sound pressure nodes. This indicates that the air molecules are moving at an extremely fast rate at this location.

Bernoulli forces emerge in consequence of this movement, which hold the drop radially [11, 13].

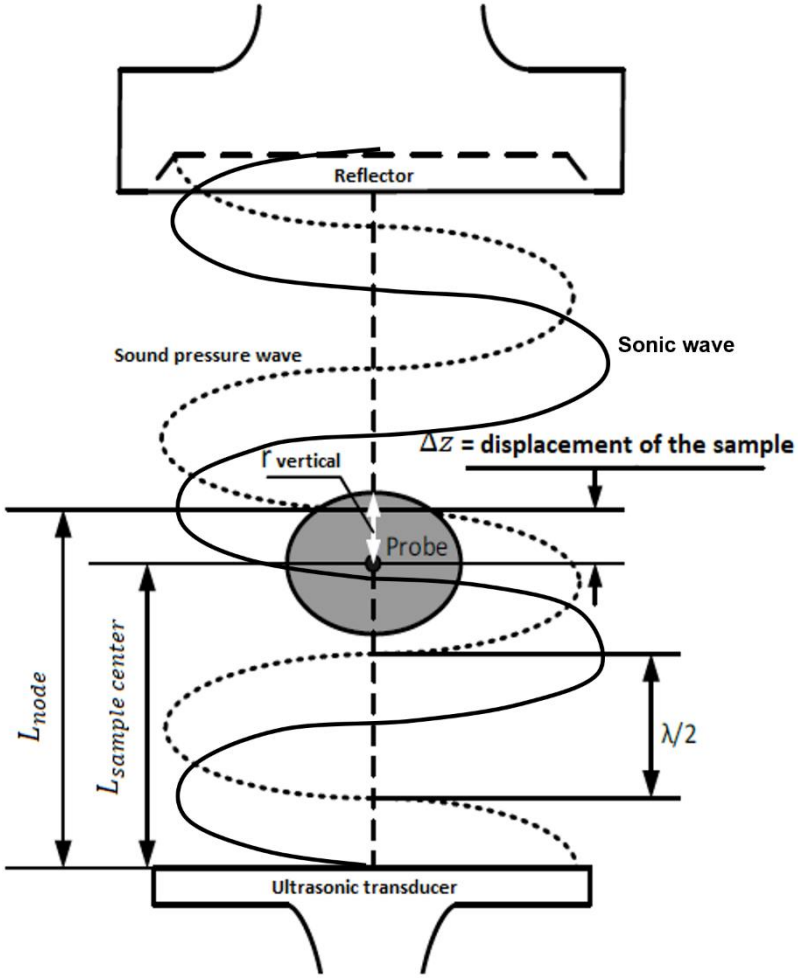

Figure 2.1 A Standing Ultrasonic wave [1]

In a standing sound field, there are two components to the overall acoustic placement force. The axial force represents the pressure component of sonic radiation F_z, while Bernoulli describes the negative pressure component F_R. The axial positioning force $F_{ax} = F_z$, which directs along the levitation axis z, compensates the gravitational force acting on the sample. The radial force F_R, which is perpendicular to the axis of levitation, does not compensate for the sample's weight in a significant way. It does, however, prevent the sample from migrating out of the pressure node in the lateral axis. As a result, the force F_R is critical for the levitated sample's stability. Figure 2.2 illustrates an acoustically levitated drop with forces acting on it [11, 13].

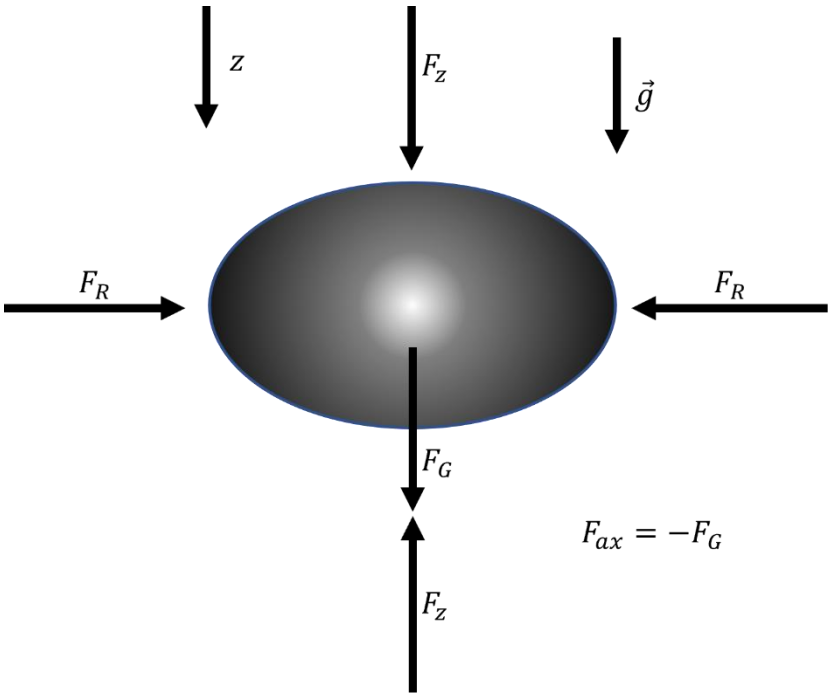

Figure 2.2 Acoustic forces acting on a liquid drop [14]

The axial positioning force for a spherical and sound-hard sample with the volume V_s, density ρ_s, and diameter d_s is obtained by integrating the axial gradient of the sound pressure distribution over the entire sample surface [11, 13].

$$F_{ax} = \frac{5}{8} k_0 \rho_0 \hat{v}_{max}^2 \cdot V_s \cdot f_1(x) \cdot \sin(2k_0 \Delta z) = \rho_s \cdot V_s \cdot g_0 \tag{2.2}$$

Here, ρ_0 is the density of the carrier medium in the static pressure distribution and the gravitational acceleration is g_0 (in $\frac{m}{s^2}$). The wave number k_0 is described by the ultrasonic frequency f (in Hz) and sound velocity c_0 in the surrounding medium (in $\frac{m}{s}$) or by the wavelength λ_0 (in m) in the following expression [11–13]:

$$k_0 = 2\pi \cdot \frac{f}{c_0} = 2\pi \cdot \lambda_0 \tag{2.3}$$

The geometer function $f_1(x)$ is defined as:

$$f_1(x) = \frac{3}{x^2}\left(\frac{\sin x}{x} - \cos x\right) \; and \; x = k_0 d_s \tag{2.4}$$

The coordinate z is counted from the reflector $(z = 0)$. The displacement Δz as can be seen from Figure 2.1 is the distance between the pressure node and the center of mass of the sample. As mentioned above, the specimen is position slightly below the pressure node. This is the result of gravitational force pulling the drop downwards during levitation. With equation (2.5), the distance between a levitated particle's center and the nearest sound pressure node can be determined mathematically [11] or by subtracting the two lengths according to Figure 2.1:

$$\Delta z = \frac{1}{2k_0}\arcsin\left(\frac{8}{5}\frac{\rho_s g_0}{\rho_0 \hat{v}_{max}^2 k_0 f_1(x)}\right) = L_{node} - L_{sample\ center} \tag{2.5}$$

The use of acoustic levitation has primary been for scientific research. Droplet drying investigations using acoustic levitation could provide a container-free environment for studying liquid evaporation and particle production [15, 16]. For providing contactless droplet manipulation, acoustic levitation has proven to be a valuable tool in container less chemistry. Acoustic levitation has been successfully used to suspend samples without the use of a container for distant analysis [3]. Synchrotron [17–20], x-ray [21–23], and Raman spectroscopy [24–26] investigations have all harnessed its advantages. Under ambient pressure, acoustic levitation has been used to investigate various physical characteristic of liquids. In 2006, Lee studied the measurement of heat capacity and thermal diffusivity using acoustic levitation. [27] Furthermore, under pressure, acoustic levitation is applied to study phase equilibrium of squalene – CO_2 system [28], mass transfer coefficient of water droplets in CO_2 [29], and measurement of density, viscosity, and interfacial tension of various saturated liquids – CO_2 [2] . Measurement of density, surface tension and viscosity has also been carried out with the help of acoustic levitation [2, 30–32].

2.2. PROPERTIES MEASUREMENT WITH ACOUSTIC LEVITATION

Measurement of physical properties using acoustic levitation has been studied theoretically and experimentally for a long time. Density of liquid particles measurement was investigated by Achatz1978 [30] and Trinh1995 [32] by acoustically levitated a drop sample in air. The required acoustic force to position a drop of a reference material is compared to the required acoustic force to levitate a drop of an unknown substance to determine density. Achatz1978 [30] also outlines how to determine density by comparing the acoustic forces necessary to place a drop of the reference material and an unknown substance at the exact

same levitation position. For measurement of surface tension, Achatz1978, Apfel1993, and Trinh1995 studied a method using shape oscillations of an acoustically levitated drop experimentally [30–32]. Hsu1987 and Marston1980 studied this method theoretically [33, 34]. Shape oscillations of acoustically levitated drops has also been investigated experimentally and theoretically to determine the drops' viscosity [30–32, 34].

For measurement of physical properties under pressure, Kremer2018 investigated acoustic levitation methods to determine density, interfacial tension, and viscosity of several binary system of liquid drops in a gaseous or supercritical CO_2-environment [2]. The methods were first validated under ambient pressure before transferring to a high-pressure acoustic levitator plant. Then the obtained results from the acoustic levitation methods are compared to conventional methods from literature data or experimental results. For density, the results are compared to data attained from a vibrating-wire viscometer. For interfacial tension, data from acoustic levitation methods is compared with literature value achieved with capillary rise method and the pendant-drop method. Viscosity data is compared to literature data using a falling body, a capillary viscometer, and a vibrating-wire viscometer [2]. Although measurement of physical properties utilizing acoustic levitation poses some limitations, it can be a reliable method for investigating liquid particles without contacting the sample physically.

2.3. IMAGE ANALYSIS

For carrying out the properties measurement as described in section 2.2, shape oscillations of an acoustically levitated drop are analyzed by taking pictures of the levitated sample and process them in an image processing software. One possible analysis is developed by Kremer2018 [2] using Matlab© to analyze the images recorded during measurement. The provided Matlab© program is used for the experiments which are carried out during this thesis. Therefore, it's functionality is explained in this chapter.

A drop of an unknow liquid is stimulated into shape oscillations to determine its interfacial tension and viscosity. The drop displays a damped oscillation when the excitation signal for these oscillations is turned off, which may be observed with a high-speed camera. The length of 1 video is approximately 1.8s which contains 3600 images. The video is then cropped so that only the useful footage remains, which usually contains around 450-650 frames. Images

are saved as bitmap format (bmp) and analyzed in a loop. The analyzation result measures the volume of the drop and the radii from the drop's contour and derives the frequency of oscillation and the damping constant from the free decay. First, the contour of the backlit drop can be described by changing the intensity value of the image. Then, the volume and radii of the drop are computed. The volume can be determined by splitting the drop into cylindrical disks. Prior to determining the volume, a calibration step utilizing a precision ruby sphere is executed to estimate the length of one pixel. The measured equatorial and polar radius of the drop are fitted to the equation of a damped harmonic oscillator to calculate the frequency and damping constant. The code consist of five sections: *calibration*, *edge detection*, *transformation of principle axes*, *volume and radii determination*, and *curve fitting process* [2].

Calibration

The length of pixel must be determined in order to obtain the drop dimensions in metric units from the recorded image. To determine the pixel length, image of a precision ruby sphere with a diameter of 2 ± is analyzed. An image of the sphere is captured, and its horizontal and vertical dimensions are measured in pixels. The length of one pixel is calculated by dividing the notional diameter of the sphere by the measured dimensions in pixels [2]. The length of 1 pixel is around 0.003mm for setup under pressure. Figure 2.3 Presents an image of the precision ruby sphere.

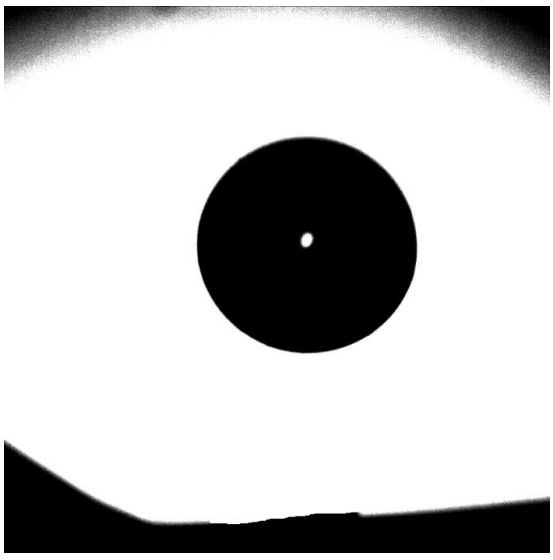

Figure 2.3: Image of precision ruby sphere

Edge detection

By tracing the horizontal and vertical radius through the drop oscillation can be monitored. Edge detection is used to determine the drop shape from high-speed photos. Two different edge detection algorithms are utilized depending on the picture noise level: THRESHOLDING or edge detection with a particular EDGE OPERATOR. An image of the afore mentioned precision ruby sphere with a diameter of 2 ± 0.0025 mm is used to evaluate each edge detection method [2].

There are two methods of edge detection: THRESHOLDING and EDGE OPERATOR. With both methods the shape of the drop can be determined. The edge operator is however unable to work effectively under high pressure. The detected edge does not match the actual drop contour due to a blurry drop contour. Furthermore, when the pressure rises, the picture noise increases. This noise is recognized as edges by the code using an edge operator, and the noise is too large to be eliminated using the described approach [2]. Since the commissioning of an acoustic levitator in this thesis is only concerns high-pressure environment experiments, only the thresholding methods is relevant during the image processing step.

THRESHOLDING uses a threshold value to split an image into foreground and background. The image is segmented by setting all pixels with luminescence levels greater than the threshold value to one (white), and the rest to zero (black). The threshold values can be adjusted manually based on the image's brightness in the Matlab© code. The drop's contour is then derived from the resulting image. An example of drop's contour (in white) on a black background is presented in Figure 2.4. Since the contour is made up entirely of perimeter pixels, it is not smooth [2].

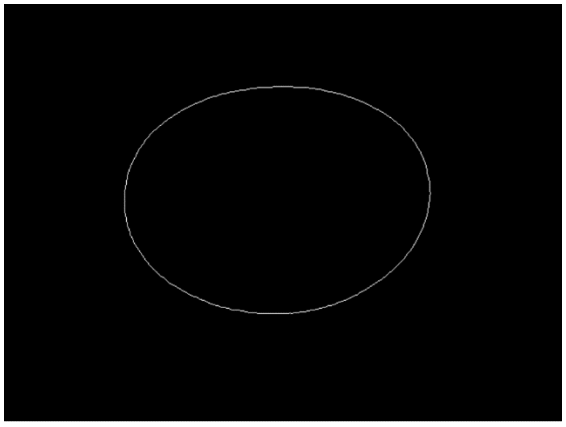

Figure 2.4: Contour of a drop

Transformation of principal axes

To determine the drop's volume, the origin of the coordinate system must coincide with the center of the drop. Additionally, the drop must be axially symmetric to the vertical axis. In some cases, the drop is tilted, depending on its size and the reflector position. Moreover, the initial coordinate system provided by the Matlab© code has its origin in the lower left corner of the image. Therefore, a transformation of the principal axis is needed. After edge detection, the drop contour' coordinates (x, y) are saved in a matrix A. Then the drop contour is shifted in two stages. First, the origin is relocated to the center of the drop. For each image, the drop center's position (m_1, m_2) (Figure 2.5) is determined. Then, the new coordinates (x_i, y_i) with i = 1, …, n are obtained by subtracting the mean values for m_1 and m_2 from every point of the drop contour and saved in a second matrix B. Afterwards, the drop contour is rotated by a transformation of the principal axes, so that the drop's minor axis coincides with the vertical axis [2] as shown in Figure 2.5.

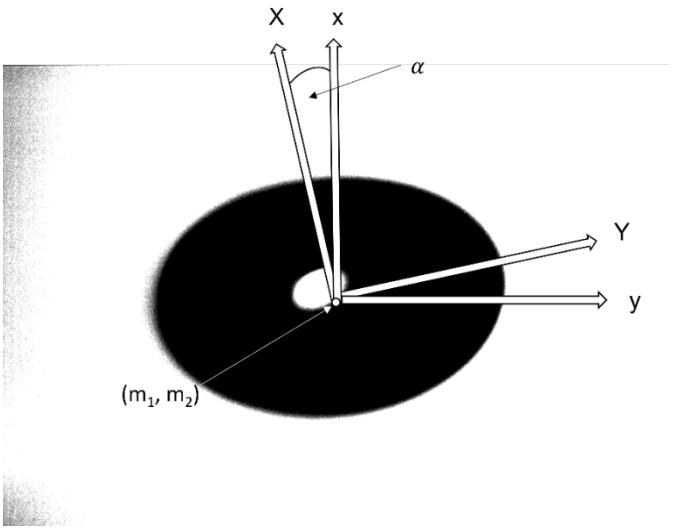

Figure 2.5: Tilted drop with shifted (x, y) and rotated coordinate system (X, Y)

From the shifted coordinates, a covariance matrix K is calculated and expressed as follow [2]:

$$K = B \cdot B^T \tag{2.6}$$

$$B = \begin{bmatrix} x_1 - m_1 & y_1 - m_2 \\ \cdots & \cdots \\ x_n - m_1 & y_n - m_2 \end{bmatrix} \tag{2.7}$$

The eigenvectors of the covariance matrix K and the original matrix B are used to calculate the rotation angle α. The coordinate system is then rotated to satisfy the equation 2.8 [2].

$$\begin{bmatrix} X \\ Y \end{bmatrix} = \begin{bmatrix} cos\alpha & sin\alpha \\ -sin\alpha & cos\alpha \end{bmatrix} \cdot \begin{bmatrix} x \\ y \end{bmatrix} \tag{2.8}$$

After executing the mentioned processes, the drop is ready for volume determination with the origin of the new coordinate system is in the center of the drop and the drop is axially symmetric to the vertical axis

Volume and radii determination

The equatorial and polar radii and the volume are determined for every image. The drop contour is saved in a matrix $[X \quad Y]$. As a result, the horizontal radius is half the difference between the maximum and minimum value of the x-coordinates, while the vertical radius is half the difference between the maximum and minimum value of the y-coordinates.

The drop shape is considered to be axially symmetric to the vertical axis for volume calculation. Therefore, the coordinate system's origin is in the drop's center, dividing it into two parts along the vertical axis (Figure 2.6).

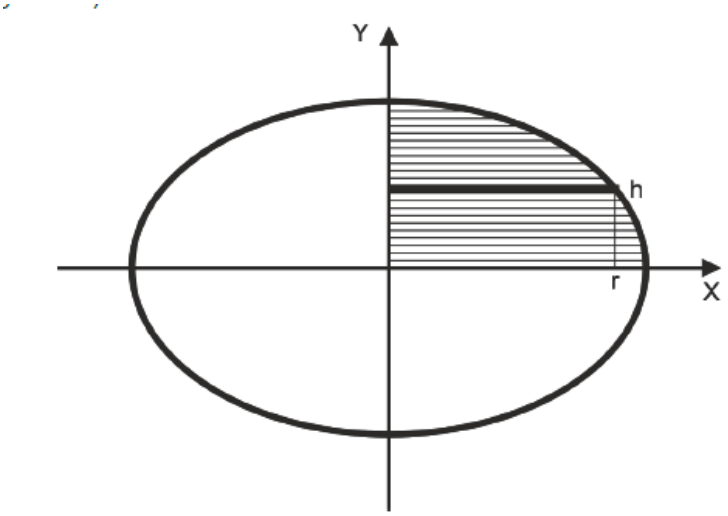

Figure 2.6: Volume determination [2]

To determine the volume of the right-hand side of the vertical axis, the volume V (in µl) of each cylindrical disk is calculated using equation 2. With the radius r serving as the value of the x-coordinate, while h (in m) represents the height of one pixel. The volumes are then summed up to acquire the right-hand side's volume [2].

$$V = \pi \cdot r^2 \cdot h \tag{2.9}$$

The method is repeated for the left section of the drop (Figure 2.6). The volume of the drop is computed by averaging the volume of the left-hand side section and the volume of the right-hand side section of the drop.

This procedure is repeated for the part on the left-hand side of the drop (Figure 2.6). The volume of the entire drop is calculated by averaging the volume of the part on the left-hand side and the volume of the part on the right-hand side of the drop. This process is carried out for each and every image in the high-speed recording [2].

Curve fitting process:

The development of the drop radii is tracked throughout time after volume and radii determination of the drop. The experimental data for the radii are plotted with time and fitted to the equation of a damped oscillator to obtain the damping coefficient and frequency of oscillation. The beginning point of the damped oscillation must be established automatically by Matlab© prior to fitting. Afterwards, the evolution of the drop radii $r_{e,p}$ (in mm), with e, p stands for equatorial and polar respectively, over time t (in s) is fitted to the following equation.

$$r_{e,p}(t) = A \cdot e^{-\tau \cdot t} \cdot \cos(2\pi \cdot f \cdot t) + r_{e_0,p_0} \tag{2.10}$$

The dimensionless amplitude of oscillation A, damping constant τ (in $\frac{1}{s}$), oscillation frequency f (in Hz), and droplet radii in rest r_{e_0,p_0} (in mm) are all fitted. The non-linear least squares fitting approach is employed, which is already implemented in Matlab©. For further processing, the findings are stored in an Excel file.

3. ACOUSTIC LEVITATOR SETUP

In the following chapter, the experimental apparatus and its function is described in detailed. Afterwards, current limitations and restricts of the setup is pointed out.

3.1. EXPERIMENTAL SET UP

The acoustic levitator for contactless sample investigation is made up of two essential components: an ultrasonic sonotrode and a reflector. Figure 3.4 illustrates a commercially used ultrasonic sonotrode that has an ultrasonic transducer at the bottom and an ultrasonic horn at the top.

Figure 3.1 Ultrasonic sonotrode [1]

The ultrasonic transducer can be excited piezoelectrically by the piezoceramics making use of the indirect piezoelectric effect. The indirect piezoelectric effect describes the deformation of the material along an axis caused by a voltage application. The indirect piezoelectric effect is utilized to set the frequency and amplitude of the piezoceramic oscillation to a specific value. By varying the frequency and the amplitude of the applied voltage to the piezoceramic, they can be excited to the desired oscillation. This oscillation will the create vibration which is transferred to nearby metal bodies. As a result, the vibrating metal bodies excite the molecules in the surrounding gaseous medium, resulting in the generation of sound waves as stated in section 2.1. This set up is called a Langevin transducer.

For the investigations, an acoustic levitation system including an acoustic levitator, signal production device, a high-speed camera (CR 3000x2, Optronis, Germany) with a tele converter and a macro-objective (EX 2.8/105 DG Macro NAFD OS HSM and TC-2001, Sigma GmbH, Germany), a light-emitting diode (LED) light source, and a computer for data accessions was employed. An Arbitrary Function Generator (AFG-2112, GW Instek, China) powers the transducer. The voltage of the radiated waves is increased by a 2 Channel Isolated Amplifier (33502A, Keysight Technologies, USA) to maximize the levitation force.

The transducer and reflector are installed in a high-pressure view cell (New Ways of Analytics, Germany) for pressures up to 16 MPa and temperatures up to 433 K for high pressure measurements. The high-pressure acoustic levitator is illustrated in Figure 3.5. [2]

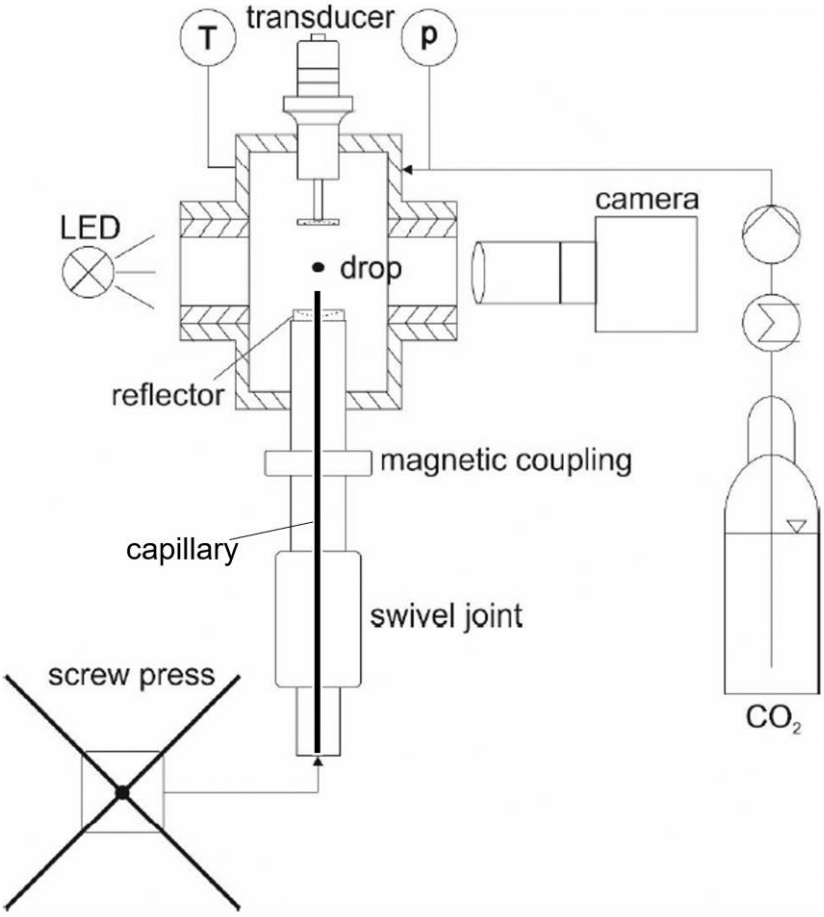

Figure 3.2 Scheme of the high-pressure acoustic levitation system [2]

In the high-pressure view cell, the transducer and reflector are place opposite of each other along the gravity axis, so that the emitted ultrasonic waves are reflected on the concave surface of the reflector. A magnetic coupling is used to manually change the distance between the transducer and the reflector. Depending on the temperature and pressure within the view cell, a stationary sound field is generated at frequencies ranging from 31 to 39 kHz by the transducer. To regulate temperature inside the view cell, a PT100 (PT100 A 15/10, ES electronic Sensor GmbH, Germany) in conjunction with a temperature controller (HT MC1, Horst GmbH, Germany) was installed. The pressure is monitored by a pressure sensor (S11, Wika, Germany) connected with a display (GRA 0420 VO, Greisinger, Germany). A capillary

penetrates through a central hollow tube in the reflector and injects the drop. A swivel joint moves the capillary along the axis of levitation. A drop on the capillary's tip is manually created using a screw press (High Pressure Equipment CO. Inc., USA). [2] A PTFE tube is inserted above the syringe needle to assist the drop detachment process.

3.2. FUNCTION

The high-pressure acoustic levitator set up is applied to measure physical properties of liquid under high pressure. In this section, the function of the acoustic levitator is presented. The high-pressure plant can inject a drop of sample into a sound field and levitate it. Then, the sample is excited to oscillation. During the measurement, visual observation of the drop is provided, and the backlit drop images are captured. Throughout the levitation process and the oscillation process, the sample might fall onto the reflector surface, disrupting the process. Therefore, demounting and cleaning of the setup is essential for the measurement process. Figure 3.3 illustrates the high-pressure acoustic levitator plant.

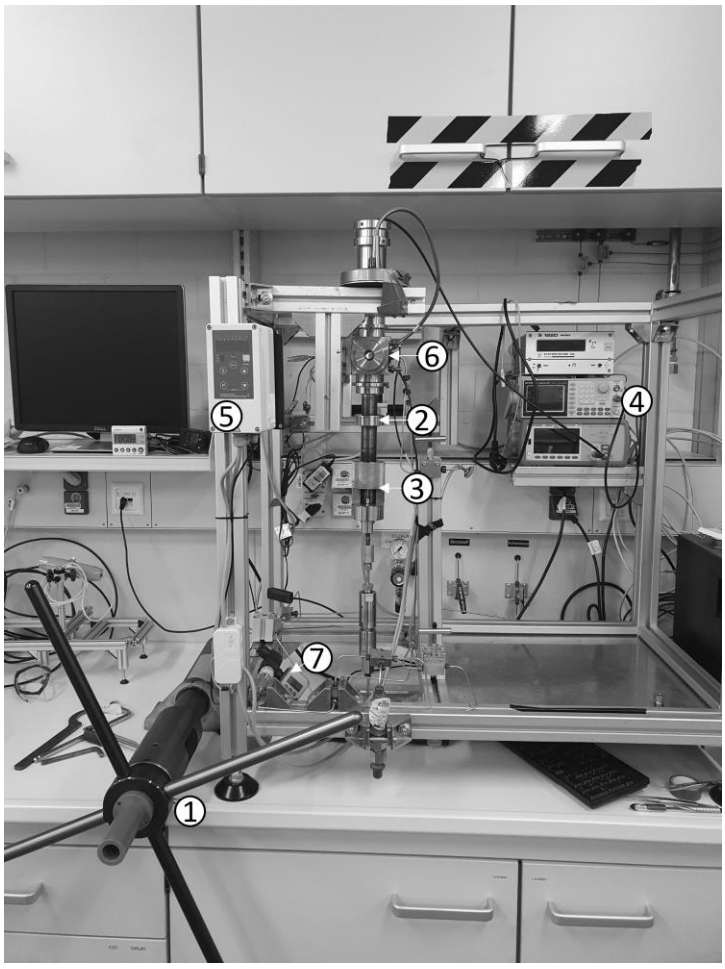

Figure 3.3: Realistic view of the high-pressure acoustic levitator setup

Components of the high-pressure acoustic levitator setup: (1) screw press, (2) magnetic coupling, (3) swivel joint, (4) wave generator, (5) PID controller, (6) view cell, (7) S11 pressure sensor

Drop injection:

To inject a drop into the sound field, the reservoir is first disconnected from the system to ensure there is no air inside the capillary during the refilling process. Then, the reservoir is filled with a desire liquid. If the wanted liquid is different from the previous one, the reservoir and the pipes must be emptied and clean thoroughly. After the reservoir is filled, reassemble the system and start turning the screw press (1) slowly. A drop will slowly emerge at the tip of the capillary.

Drop levitation:

Temperature and pressure affect sound speed inside the host medium. As a result, the levitation frequency must be adjusted at the wave generator (4) to figure out the transducer's eigenfrequency. Next, a magnetic coupling (2) is used to alter the distance between the transducer and the reflector. When resonance conditions are met, a swivel joint (3) can be used to move a capillary through a hole in the reflector until a PTFE tube emerge from the reflector's surface. Using the screw press, a drop is injected and placed into a pressure node. The distance between the transducer and the reflector is regulated again slowly until the drop is pulled out of the capillary. For the stabilization of the levitation, the capillary is carefully removed from the acoustic field. Since removing the capillary will slight effect the reflector position, causing the sound field to be unstable, and therefore the drop is shaky. It is crucial to adjust the position of the reflector again using the magnetic coupling (2) to ensure stabilization of the drop. Figure 3.4 shows the reflector housing with the magnetic coupling and the capillary with the PTFE tube at the top.

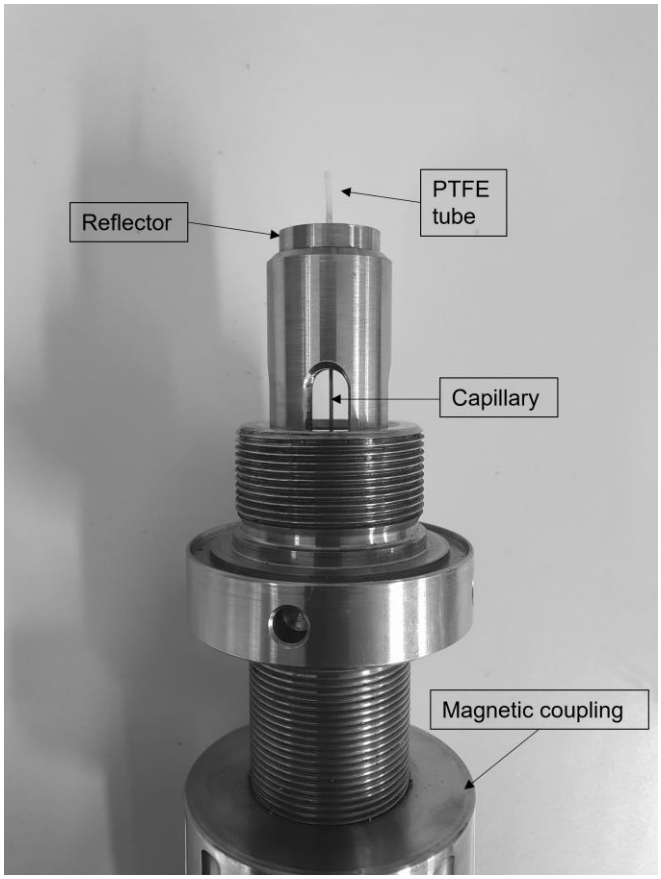

Figure 3.4: Detailed view of the reflector housing and the capillary located inside

Drop oscillation:

To excite a drop to oscillation state, the stably levitated drop is introduced to a low frequency amplitude modulation (AM) of the high intensity transducer drive signal. Before drop injection, AM is setup at the frequency generator to a specific modulation depth and frequency which varies depends on the viscosity of the examined liquid. AM is turn on only after the drop is successfully introduced to the sound field and stably levitated. Then a clear visible oscillation appears.

Pressurizing the system:

Pressure is increase by flushing CO_2 in the autoclave through an inlet valve. Pressure is monitor through a sensor (7).

Temperature control:

The heating of the high-pressure viewing cell is carried out via four heating cartridges. The temperature of the inner environment of the cell is measured with a PT100 thermo sensor,

which is connected to a PID controller (5) to regulate the temperature inside the view cell. The view cell is heated up to the desire temperature in steps of 5K.

Visual observation of the specimen:

Specimen can be observed through a sapphire glass of a high-pressure view cell (6). The view cell is cross-shaped and can handle a maximum pressure of 150 bar at a temperature of 180^{o}C. Figure 3.5 depicts the side view of the cross-shaped view cell.

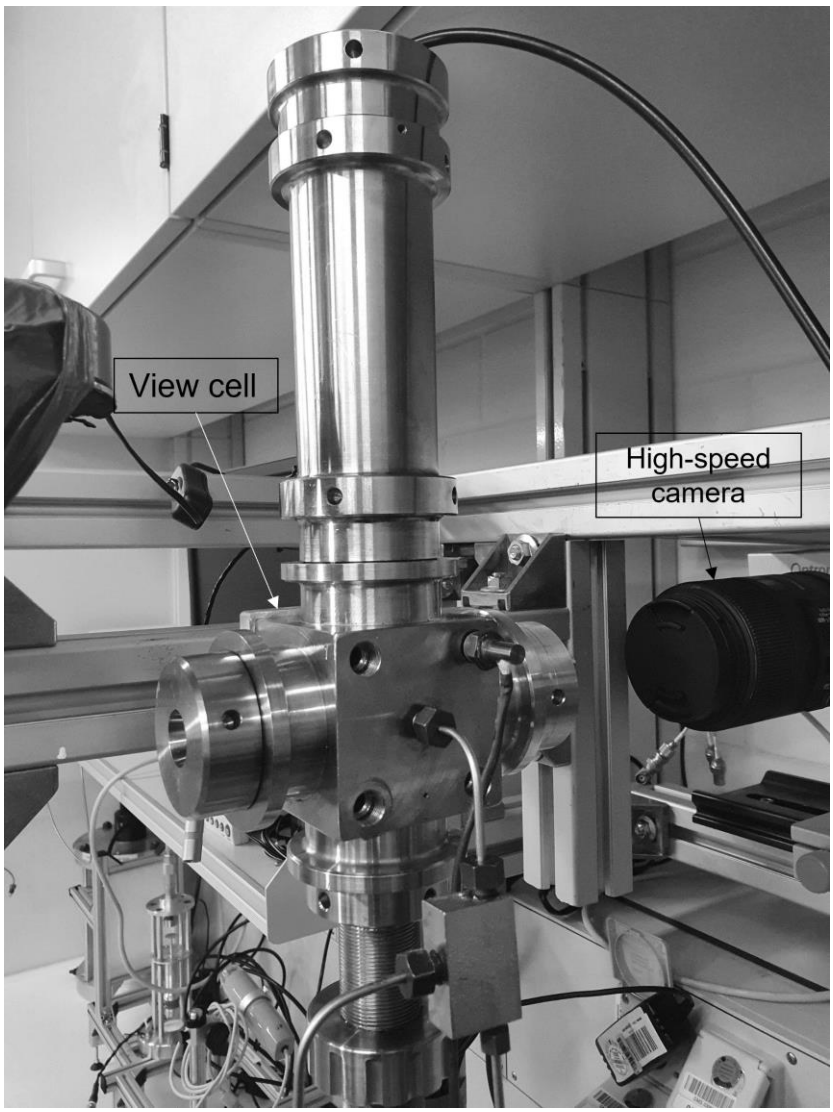

Figure 3.5: High-pressure view cell with high-speed camera

Record the process visually:

Shadow images of the specimen can be observed and recorded with a high-speed camera with 2000fps.

Demounting and cleaning:

After each experiment, parts of the plant must be removed for cleaning. First, pressure must be released complete with an exhaust valve. Then, the autoclave is opened in the front to access the reflector. Next, the reflector surface is cleaned carefully with a cotton bud to avoid damage such as scratches or crack. The surface can be cleaned using ethanol or distilled water depending on the previously investigated liquid. If the next experiments use a different liquid than the previous one, repeat steps in the ‚drop injection '. If not, reassemble the view cell and continue with the experiments. During the pressurizing process, the pressure does not stabilize but decreases with time. This is a result of leakage inside the system. Leakages can possibly occur at the O ring inside the front view door (8) and the lower area reflector housing (9) is damage due to contact with high pressure CO_2. As a results, CO_2 might leak through these parts. Replacing the O ring inside these components should fix the problem in most cases. Figure 3.6 shows the positions of the O rings that might occur leakage.

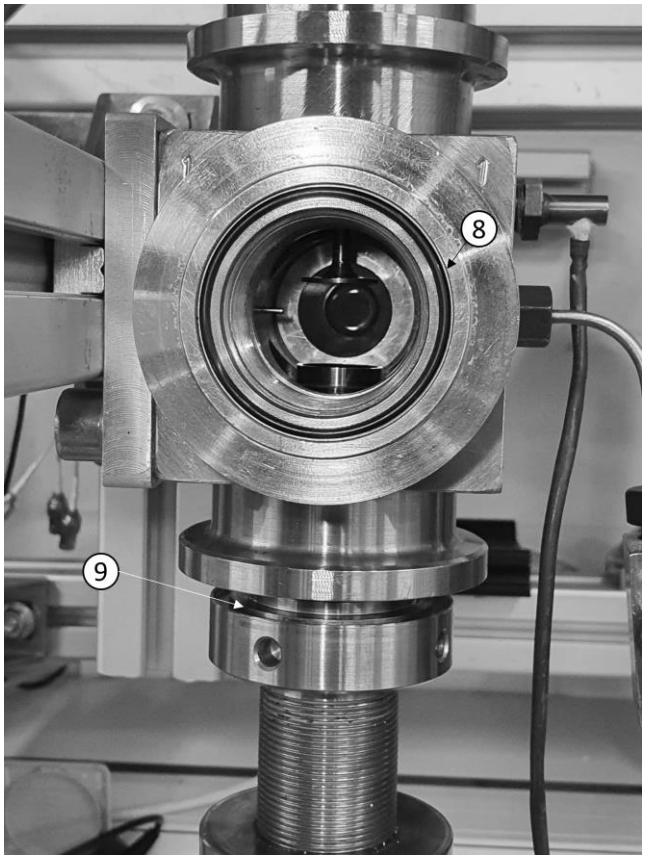

Figure 3.6: Front of the viewcell and the lower part of the reflector housing

Components: (8) O ring of the front view cell door, (9) O ring of the lower part of the reflector housing

3.3. LIMITATION AND RESTRICTIONS

The current setup possesses many limitations that interfere with its operation. First, to pressurize the system, the plant is heated in 5K step to the desire temperature. Then CO_2 is flushed into the cell. Then, pressure and temperature slowly stabilize. Afterwards, pressure is adjusted again until the desire value is reached. This process can be repeated a several times consuming a considerable amount of time. In case the system needed to be depressurize for cleaning or changing the experimental material, then the measurement process would be interrupted for a significant amount of time. This limits the number of experiments that can be performed in a period of time e.g., day or week. To levitate a sample, resonance conditions must be reached. However, the resonance frequency changes with each temperature and pressure due to the different in sound speed. The plant does not indicate when resonance is reached, the eigenfrequency is therefore cannot be found easily and must relied on experimenting or previous data. Sample is placed into a pressure node for levitation. The pressure node, however, cannot be indicated clearly. Consequently, it is impossible to levitate different samples at the same pressure node. Next, volume of the produced drop cannot be determined since the screw press does not have any indicator on it. Thus, the measurement results might be unreliable. While removing the capillary, the reflector also moves since they are connected (see Figure 3.4), this destabilizes the levitation and might cause the drop to fall. If the drop does not fall, with the misaligned reflector and transducer, the sound field is altered, causing the drop's center to shift away from the levitation axis in a radial direction. This results in the drop leaving the focal region of the high-speed camera, creating a blurry image. Moreover, the drop temperature, which is important in the analysis of the liquid, cannot be monitored while being levitated under pressure. With the current setup, the temperature sensor can only determine the temperature of the fluid near the drop but not the drop itself. In addition, after 5 to 6 experiments, the drops that fell onto the reflector previously prevent the reflecting of the sound waves. Consequently, it is impossible to proceed with the experiment. The system is then depressurized, the reflector has to be cleaned before the heating and pressurizing process happens again. This leads to a significant waste of time. The same frequency and distance of the transducer from the reflector cannot be replicated in every experiment, since with each injection and capillary removal, the reflector position changes. Furthermore, the present apparatus poses restrictions. A

difference in density or compressibility between the host fluid and the levitated liquid is necessary to accomplish levitation. The CO_2-density limit with the described system is 630 $\frac{kg}{m^3}$. The acoustic force is insufficient for levitation at higher densities of the host fluid. Another limitation is caused by using of a capillary and a swivel joint for drop injection. The force required to spin the swivel joint rises as the pressure increases. Manual rotation of the swivel joint is nearly impossible at pressures exceeding 120 MPa [2]. The setup provides a new method to measure physical properties under high pressure. However, with the current limitation, to acquired reliable results the measurement must be carefully performed with extreme care to detail.

4. COMMISSIONING AND EXPERIMENTS

In this chapter, the commissioning of the acoustic levitator is presented. After the proper methods of density, interfacial tension, and viscosity measurement are reviewed, the measurements of these properties are carried out under elevated pressure (up to 80 bar) without wall contact. Afterwards, the obtained results are presented and discussed.

4.1. MEASUREMENT OF DENSITY

4.1.1. METHODS

A drop is levitated by acoustic levitation force by applying voltage to a transducer to generate ultrasonic waves. If the voltage provided to the transducer is decreased, the acoustic levitation force also reduced. The drop form grows more spherical as the acoustic force is reduced, until the sample drops out. Figure 4.1 shows relation between the shape of the drop, expressed by the ratio of equatorial to polar radius and the levitation voltage applied at the transducer [2].

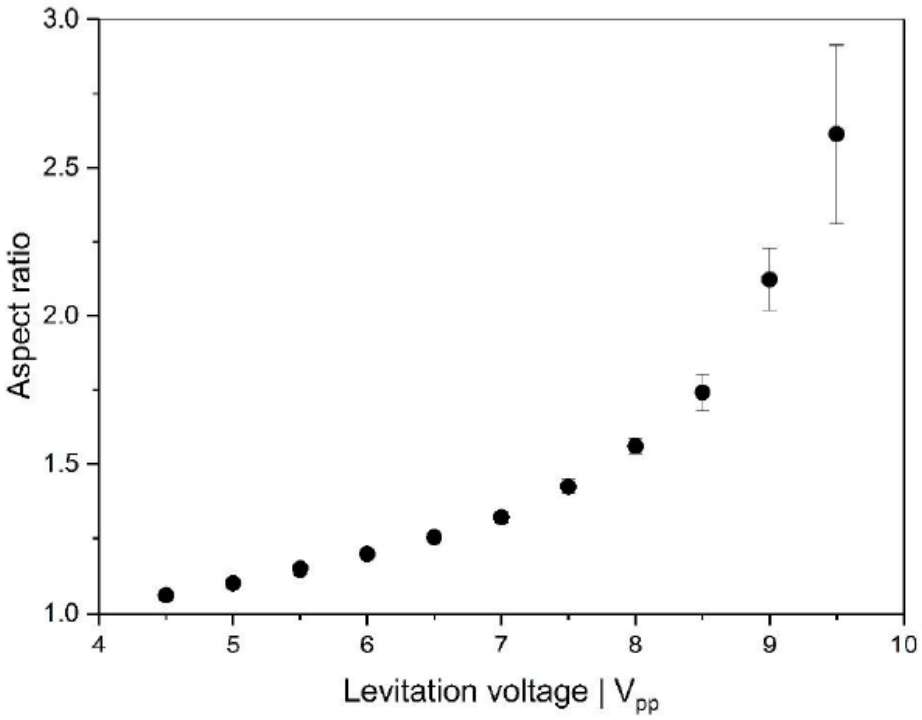

Figure 4.1: Aspect ratio against levitation voltage [2]

The aspect ratio approaches one when the levitation voltage is reduced. This represents the state of a perfect sphere. No spherical form can be achieved with ground-based acoustic

levitators, however. The aspect ratio of the drop is proportional to the levitation voltage and hence the intensity of the acoustic field. In addition, when the levitation voltage is reduced, the drop's center travels in the direction of gravity [2], as shown in Figure 4.2.

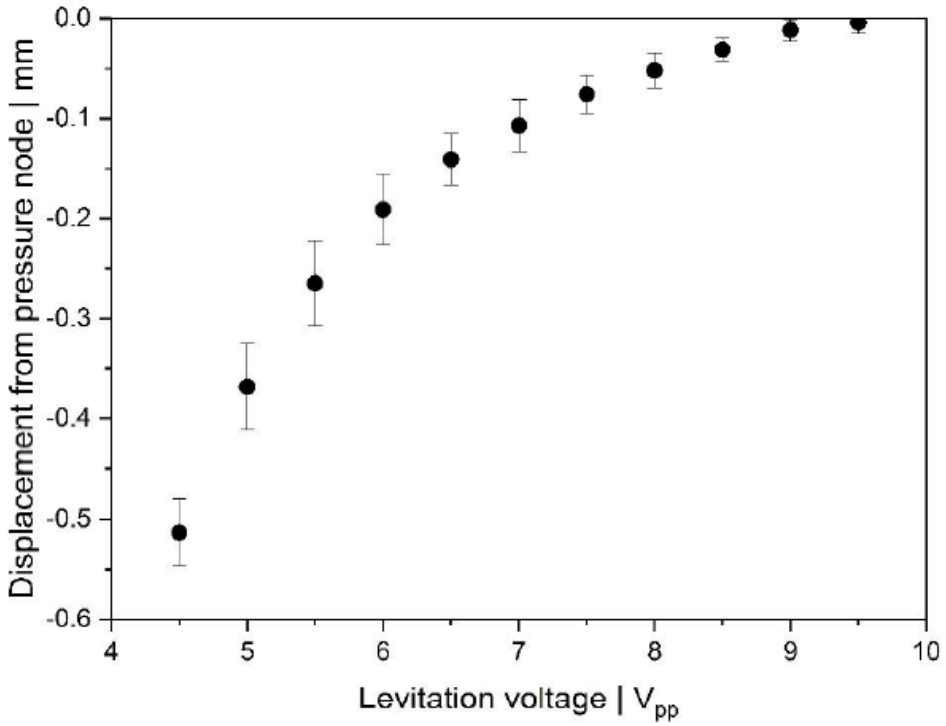

Figure 4.2: Displacement from pressure node versus levitation voltage [2]

The drop's center moves away from the pressure node in an exponential pattern as the levitation voltage decreases. The axial acoustic levitation force F_{ax} (in N) barely counteracts the sample's gravitational attraction at the moment of drop out, as expressed by equation (2.2) [11]. The acoustic force at the point of drop out solely depends on the density of the liquid for droplets of the same volume levitated under the same sound field circumstances [32].

To measure density using acoustic levitation, a drop of an unknown liquid is levitated stably in a pressure node of the standing sound field. The voltage applied to the transducer is decreased until the drop falls out of the sound field and measured. Then, a drop of a reference material with known density is levitated in the same pressure node and the voltage is reduced again. The frequency of the transducer is kept constant, as is the distance between the transducer and the reflector. Density of is determined by comparing the voltage needed to

levitate a drop of an unknow liquid (index 1) to the voltage required to levitate the a drop of a reference material (index 2) using equation (4.1) [32].

$$\rho_1 = \rho_2 \cdot \left(\frac{U_1}{U_2}\right)^2 \tag{4.1}$$

With ρ is the density of the liquid. While U, is the voltage needed to levitate the sample of the reference or unknow material respectively. The droplets must be the same size or less than 10% of the wavelength for this comparison [32]. The acoustic force of different-sized drops is also affected by the volume of the drop, the distance between the drop's center and the pressure node, and a geometry factor. Since the exact location of the pressure node is uncertain, the displacement of the drop's center from the pressure node cannot be determined using the provided setup [2].

4.1.2. PROCEDURES

For density measurement using acoustic levitation under pressure, the cell is first heated up and pressurized to the desired experimental temperature and pressure. Then, a drop is injected and levitated. Then, the levitation amplitude is slowly decreased in steps of 0.01 V_{pp} until the acoustic levitation force is smaller than the gravitational force: the point of drop out. The amplitude of the levitation and the distance between the transducer and the reflector are recorded, and the operation is repeated. With each material, ten single measurements are conducted for every temperature and pressure. The levitator is dismantled, carefully cleaned, and reinstalled after the reference material is measured. Following that, the above-mentioned process is used to measure the unknown material. The detailed setup and procedure of each step are described in section 3.1 and section 3.2, respectively. The results of the measurement are displayed and analyzed in section 4.3.

4.2. MEASUREMENT OF VISCOSITY AND INTERFACIAL TENSION

Surface tension is crucial in the formation of a new surface between two immiscible phases. A physical border forms between these immiscible phases, entirely enclosing one phase. A surface is the physical border between a liquid phase and its vapor, or between a liquid phase and air. A border between two condensed phases or one condensed and a dense fluid phase, such as a supercritical fluid, is referred to as an interface. The physical and chemical qualities of a surface differ on the interior and outside. The interaction between molecules of the same

kind is identical inside the condensed phase, and the spherically symmetrical forces operating on a molecule are neutralized. At a phase border, however, molecules only interact on one side. As a result, as shown in Figure 4.1, the resulting net force is directed inwards the phase. [35]

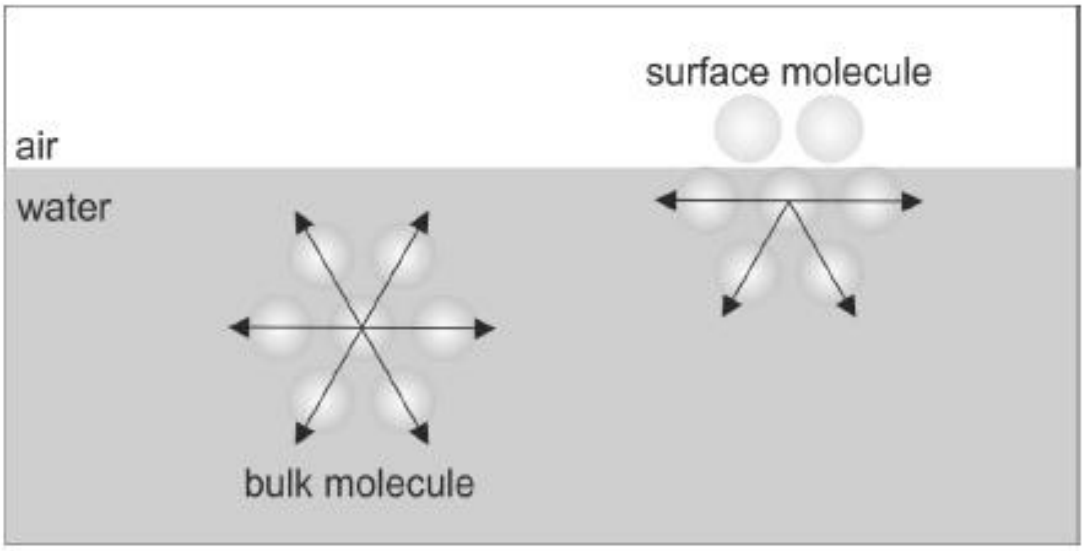

Figure 4.3 Forces acting on a molecule in the bulk phase and at a surface. [35]

To attend to the energetically most advantageous condition, a surface tends to reduce its size. The energetically most appealing form is a sphere with the lowest surface-to-volume ratio because the attracting forces of molecules at the phase boundary are directed inwards. [36]

For constant pressure and temperature, the surface/interfacial tension σ (in $\frac{N}{m}$) is the change in Gibb's free energy G (in J) per area A (in m^2) and is expressed as:

$$\sigma = \left(\frac{\delta G}{\delta A}\right)_{p,T} \tag{4.2}$$

When a new surface is generated, it takes a certain amount of time to bring the phases back into balance. It takes time for new molecules to diffuse to the surface. The observed surface tension differs from that of the system in equilibrium in this short duration, as seen in Figure 4.2. This transient surface tension is referred to as the dynamic surface tension. [36]

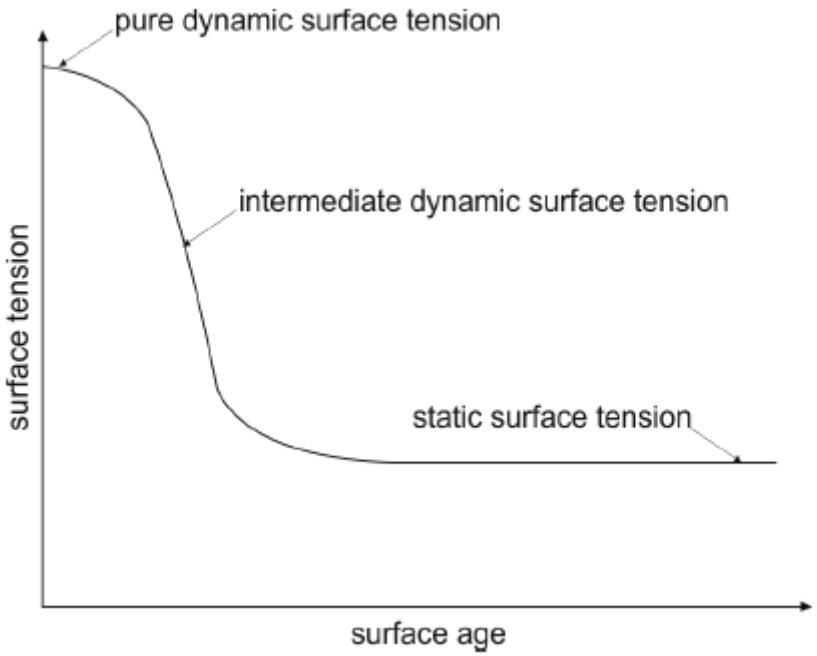

Figure 4.4: Relation between surface tension and surface age [2]

Another important attribute is viscosity, which affects spraying and droplet formation processes by influencing flow regimes. The inner resistance of a substance to flow is measured by its viscosity. A viscous fluid is represented in Figure 5.3, which is sandwiched between two infinitely parallel horizontal plates.

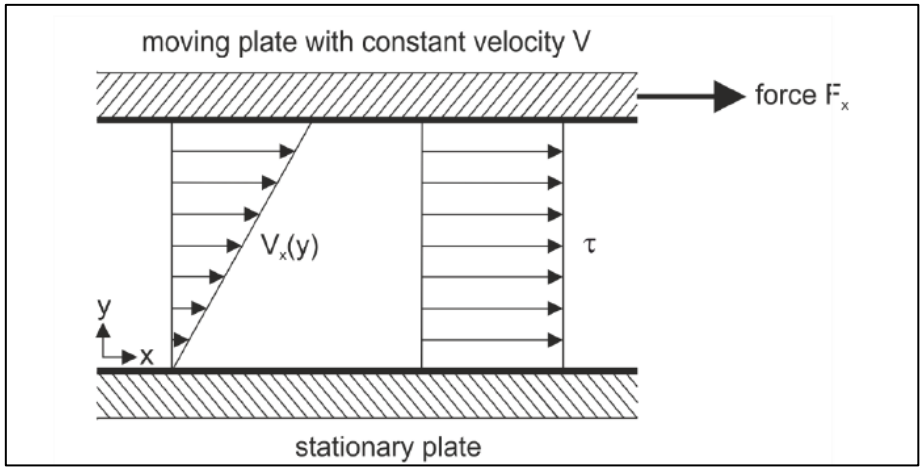

Figure 4.5: Couette flow of a fluid between two parallel plates. [2]

The viscous liquid completely fills the space between the plates. The fluid between the plates is initially at rest since the bottom plate is stationary. If a constant horizontal force is suddenly applied to the top plate, the plate moves at a constant velocity and the fluid is disturbed from its resting condition. The fluid begins to flow, forming a stationary laminar layer flow. To satisfy the no-slip condition, the fluid layer closest to the lower plate remains stationary, while

the fluid layer nearest to the upper plate travels with the same rate as the top plate. This creates a vertical (perpendicular to the axis of motion) fluid gradient across the fluid. The fluid layers begin to slip over one another at their own speeds. The layers rub against one other due to this velocity profile. To compensate for the friction created by the fluid layers and keep the upper plate moving at a constant speed, a force F_x (in N) is required. Equation 4.9 expresses the ratio between the applied force and the area of the plate A (in m^2), which is known as shear stress τ_S (in Pa). [37–39]

$$\tau_S = \frac{F_x}{A} \tag{4.3}$$

The shear stress in the Couette flow described above is constant. The shear stress is proportional to the higher plate's velocity V_x in $\frac{m}{s}$. The following equation describes the local change in velocity between fluid layers in the vertical direction. [37–39]

$$\dot{\gamma} = \frac{dV_x}{dy} \tag{4.4}$$

The shear rate τ_S (in $\frac{1}{s}$) is constant for a Couette flow in terms of shear stress. Equation 4.11 describes the relation between shear rate and shear stress. [37–39]

$$\tau_S = \eta \cdot \dot{\gamma} \tag{4.5}$$

The constant of proportionality η (in Pas) represents the liquid's dynamic viscosity and is the liquid's inner resistance to deformation. The shear stress of ideal viscous liquids is proportional to the shear rate.

Interfacial tension is expected to linearly decrease as temperature rises and increase as pressure raises.

$$\left(\frac{\delta\sigma}{\delta p}\right)_{T,A} = \left(\frac{\delta V}{\delta A}\right)_{p,T} \tag{4.6}$$

The viscosity of gases increases as the temperature rises. Liquid kinetic theory is more challenging than gas kinetic theory. Furthermore, strong intermolecular forces affect liquid viscosity and must be taken into account. A rise in temperature typically causes a reduction

in viscosity in a pure, liquid fluid. For most liquids, the viscosity of a pure material increases as pressure rises.

4.2.1. METHODS

Interfacial tension and viscosity of water with compressed CO2 is investigated. Using shape oscillations of levitated drops with acoustic force under CO_2-pressure physical properties of water can be calculated. To evaluate the accuracy of the acoustic levitation method, the attained results are compared to literature data obtained from conventional methods. The results are compared to Georgiadis2010 [40], Hebach2002 [41] who use pendant drop method and Chun1995 [42] who use capillary rise 006Dethod to determine interfacial tension of the CO_2-water system. For viscosity, results are compared to Nagashima1977 [43] who combined data from different methods such as capillary viscometry and falling drop

Acoustic Levitation using Oscillating drop

The surface tension and viscosity of an acoustically levitated drop are derived using freely decaying oscillations. Thus, an amplitude modulation of the transducer drive signal is needed to excite the drop into oscillation. A low frequency signal f_M (in Hz) is superimposed on a high frequency sinusoidal carrier signal f_C (in kHz). The amplitude of the carrier signal $U(t)$ (in V_{pp}) is altered with time by the low frequency signal sinusoidally with an initial amplitude U_0 (in V_{pp}) expressed as follow.

$$U(t) = U_0 \cdot [1 + M \cdot \sin(2\pi \cdot f_M \cdot t) \cdot \sin(2\pi \cdot f_c \cdot t)] \tag{4.7}$$

The amount by which the voltage is adjusted is controlled by the depth of the modulation, which is indicated by M. Figure 4.6 depicts the amplitude modulated transducer drive

Signal [44, 45].

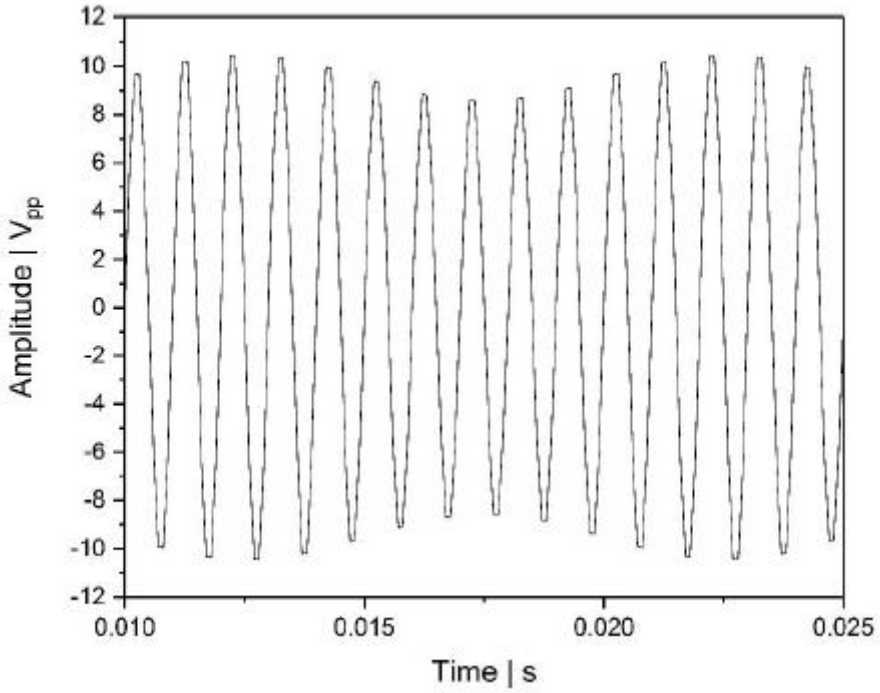

Figure 4.6: Amplitude modulation of the high frequency carrier wave [2]

The amplitude modulation is shut off, results in the drop exhibiting a damped oscillation. The surface tension determines the oscillation's frequency while viscosity controls the time until the drop reaches its equilibrium shape. In the absence of gravity, the following equations are derived for small amplitude oscillations of a spherical form drop. It is assumed that the liquid is incompressible and viscid. The host medium's viscosity and density are negligible. As described by equation (4.9), the surface tension σ (in $\frac{N}{m}$) depends on frequency of drop shape oscillation f (in Hz), mode of oscillation l, liquid's density ρ (in $\frac{kg}{m^3}$) and volume of the drop V (in m^3) [44, 45].

$$\sigma = \frac{3\pi \cdot f^2 \cdot \rho \cdot V}{l(l-1)(l+2)} \tag{4.8}$$

With the influence of the liquid's viscosity on the frequency of oscillation neglected, the dynamic viscosity is a function of the damping constant τ (in Pas), the density $\rho \frac{kg}{m^3}$, the mode of oscillation l, and the radius of a sphere with the same volume as the distorted drop R (in m) as expressed by equation (4.10) [44, 45].

$$\eta = \frac{\tau \cdot \rho \cdot R^2}{(l-1)(l+2)} \tag{4.9}$$

The radius of the volume equal sphere *R* (in m) can be calculated using the following equation.

$$R = \sqrt[3]{\frac{3V}{4\pi}} \tag{4.10}$$

It is predicted that the viscosity of the drop reduces the oscillation frequency (equation 4.12) [46].

$$f_{reduced} = \sqrt{f^2 - (2\pi \cdot (1/\tau)^{-2}} \tag{4.11}$$

The Ohnesorge number Oh is a measurement of friction force as a function of inertia and surface force. The equations above are valid only if the Ohnesorge number meets the following criteria:

$$Oh = \frac{\eta}{\sqrt{\rho R \sigma}} < 0.1 \tag{4.12}$$

These equations can only be used if the influence of the host medium is neglected. The density ρ_o of the outer host medium determines the frequency of oscillation in liquid-liquid systems. Interfacial tension and viscosity are determined using eqs. (4.14) and (4.15), respectively, for the axisymmetric fundamental mode (4.21) [47].

$$\sigma = \frac{\pi \cdot f^2 \cdot (3\rho_i + \rho_o) \cdot V}{8} \tag{4.13}$$

Additionally, the viscosity is also influenced by the host's density ρ_o and viscosity η_o [34].

$$\eta = \frac{\tau \cdot R^2 \cdot (3\rho_i + 2\rho_o) - 40\eta_o}{15} \tag{4.14}$$

4.2.2. PROCEDURES

For interfacial tension and viscosity measurement, the cell is first heated, then CO_2 is flushed in to increase pressure. Afterwards, a drop is injected and levitated as mentioned in section 4.1. Then, amplitude modulation (AM) is switched on at the desired depth of modulation to induce an axisymmetric prolate-oblate type shape oscillations to the drop. The depth of AM depends on the experiment liquid. A modulation depth of 10 % is satisfactory for water-based liquids. For liquid with higher viscosity however, a higher depth of amplitude modulation might be necessary. Then, the AM' frequency is modulated until a running mode behavior is seen on the drop. The running mode represents the overlap of the oblate-prolate

oscillation and rotation modes. Then, the frequency is decreased again until the oscillation amplitude is at is maximum. At this point, the drop is oscillating in its axisymmetric fundamental mode ($l = 2, m = 0$). This process must be done to ensure that the running mode does not occur during the damped oscillation. Since the drop is not oscillating in the eigenfrequency if there is a superposition of oblate-prolate oscillation with rotation. The transition from the running mode behaviour to the asymmetric oblate-prolate shape oscillation can be observed by eye. To create a damped harmonic oscillation, the depth of AM is set to zero, this immediately stops the amplitude modulation. At the same time, the high-speed camera is started to record the free decay of the drop. The high-speed video is reviewed immediately after recording to guarantee that no rotation happened during the damped oscillation. During the free decay, if there is rotation, the drop again displays a running mode. If rotation is found, the modulation frequency is reduced, and the experiment is repeated at a lower frequency value [48].

4.3. RESULTS AND DISSCUSSION

Before evaluating the results gathered from the acoustic levitator, the relative deviation to the literature data is computed. According to the following equation, the deviation is defined as the average absolute relative deviation D (in %).

$$D = \frac{1}{n} \cdot \sum_{i=1}^{n} \left| \frac{x_{exp} - x_{lit}}{x_{lit}} \right| \cdot 100 \tag{4.15}$$

The measured properties x_{exp} from the acoustic levitator is compared to x_{lit} is the corresponding data from literature. Finally, n is the number of conducted experiments.

4.3.1. DENSITY

The measurement of density utilizing acoustic levitation is first carried out under ambient pressure and temperature. Ten single measurements for each material are conducted. The measurement method is tested on waterglass (WG) with 7% solid content, ethanol. Distilled water is used as the reference substance. Table 4.1 compares the acoustic levitation results to the published data from Kremer2018 [2], Faria2013 [49] and Fraunhofer UMSICHT.

Table 4.1: Results of density determination using acoustic levitation

Substance	Density			
	Acoustic levitation	**Literature**	**Value**	**D**
	kg/m³	**-**	**Kg/m³**	**%**
Ethanol	802.71	Faria2013	795.45	0.91
		Kremer2018	797.15	0.70
Waterglass	1031.42	Fraunhofer	1100	6.23

Acoustic levitation method for density measurement under ambient pressure produces good result for the density of ethanol as the deviation is only 0.91 % from the literature. Acoustic levitation method is also used to measure density of ethanol and compare with Faria2013 in Kremer2018 [2]. Concerning Kremer's work, acoustic levitation method produces density that deviates 0.21 % from Faria's work. This happens since the set up to measure density in this thesis is different from Kremer2018 [2]. In Kremer's work, an external precision syringe is used to inject the measured drop into the sound field. Therefore, the volume of the tested materials is constant throughout multiple measurements. Furthermore, with this set up, the injected syringe does not interfere with the levitation process. Thus, the distance between the transducer and reflector is kept constant and the investigated drop can be injected into the same pressure node reliably. However, since the deviation is only 0.7 % larger than previous measurement using acoustic levitation, this can be considered as a valid result. On the other hand, the set up used in this thesis does not have those advantages. Since the drop is injected by a screw press, the drop volume can only be determined by eye and therefore is not reproducible. Moreover, since the injection capillary is connected to the reflector through a bottom housing, the reflector might tilt and must be adjusted to guarantee the stability of the levitation while the capillary is being removed from the sound field (section 3.2). Consequently, the same reflector-transducer varies with every experiment and thus an accurate result cannot be found. For the density measurement of waterglass, the calibrated value deviates more than 6 % from Fraunhofer UMSICHT data. Since waterglass is an uncommon substance, there is no data available on the acoustic levitation of the material. Thus, the measurement of WG's density is challenging. During the experiments, the drops are produced with different volume due to the screw press. Additionally, the distance between the transducer and reflector changes significantly between the density measurements of WG.

Finally, it is decided that it is impossible to conduct density measurements under high pressure since it is not possible to reproduce the same volume of the droplets and transducer-reflector using the current setup.

To improve the measurement of density using acoustic levitation in high pressure, it is crucial to assess the limitation. Control of the injected volume is vital to the density measurement. The displacement between the transducer and reflector should be indicated for ease of adjustment. The removal of the capillary must not change the reflector position as it would lead to a readjustment of the distance.

4.3.2. INTEFACIAL TENSION AND VISCOSITY

Interfacial tension and viscosity of water in CO_2 under high pressure and temperature is measured. The measurement is done at two different environments 4 MPa at 298 K and 8 MPa at 313 K.

The high-pressure measurements are conducted in phase equilibrium with CO_2 in gaseous or supercritical state. Phase equilibrium is needed to ensure that the measured liquid's parameters are constant during experiments. Therefore, it is critical that the system reaches phase equilibrium during the measurements. For the determination process of interfacial tension and viscosity, a drop of unsaturated liquid is first introduced into the sound field through a capillary, which is then completely withdrawn from the sound field. An amplitude modulation excites the drop into shape oscillations with an appropriate value depth, and the maximal oblate-prolate oscillation is sought. The modulation is then turned off, and the damped oscillation is captured. As a result, the period between injection and measurement for interfacial tension and viscosity determination is roughly one minute [2]. To ensure phase equilibrium is reached during physical properties measurement, tests are carried out for water – CO_2 system at temperatures of 298K and 313K and pressures of 4 MPa and 8MPa. The measurement of interfacial tension and viscosity uses drops injected for one minute and drops injected for five minutes for the system with 4 MPa and 298K, while the system 8 MPa and 313k measures the drop after one minute and three minutes after injection to make sure that the liquid is saturated. Table 4.2 illustrates the interfacial tension and dynamic viscosity measured at different time after drop injection using acoustic levitation. It can be inferred from the results, that the acoustically levitated water drops in CO_2 does not reach phase

equilibrium. Although interfacial tension values stay constant after three and five minutes, viscosity does not. This might signify that phase equilibrium is not reached after one minute. However, the inconsistent value of viscosity can also be cause by error of measurement, since in Kremer2018 [2], it is proved that phase equilibrium of acoustically levitated squalene droplets in a CO_2-atmosphere is achieved in less than one minute. Therefore, it can be assumed that phase equilibrium is reached in less than one minute for water droplets in CO_2 environment for the measurements of interfacial tension and viscosity in this thesis. However, further investigation on this point is needed.

Table 4.2: Interfacial tension and viscosity measured with acoustic levitation at different time after drop injection

Time between injection and measurement	**Pressure**	**Interfacial tension**	**Dynamic viscosity**
Min	**MPa**	**mN/m**	**mPas**
1	4.1	5.50	1.00
5	4.1	5.20	1.10
1	8.1	5.50	0.24
3	8.1	5.00	1.3

After the assumption that phase equilibrium is reached during properties determination, the experiments are carried out with the water-CO_2 system. First, the damping constant and frequency of oscillation are calculated from the image analysis of oscillating drops. The outputs of the drop shape analysis are then compared to data from the literature. The shadow images of the drop are analyzed using a Matlab© code as mentioned in section 2.3. Since both the equatorial radius r_e and polar radius r_p are used in the equation (2.10), two results for the amplitude, damping constant and frequency of oscillation are generated for each drop after the analyzation of the images. Due to temperature variations in the sound field or effects from the surroundings, the dimensionless amplitude of oscillation A, damping constant (in 1/s), and frequency f (in Hz) determined from the radii deviate from each other. [2] Table 4.3 shows the results of the picture analysis in detail.

Table 4.3: Results of image analysis

No.	Equatorial radius r_e					Polar radius r_p					V	R
	A_e	τ_e	f_e	$r_{e,0}$	R^2_e	A_p	τ_p	f_p	$r_{p,0}$	R^2_p		
-	-	1/s	Hz	mm	-	-	1/s	Hz	mm	-	µl	mm
1	0.009	26.78	126.60	0.43	0.96	0.02	30.32	126.29	0.37	0.99	0.29	0.41
2	0.009	18.89	124.08	0.44	0.90	0.02	22.69	125.18	0.38	0.90	0.30	0.42
3	0.005	22.39	131.72	0.42	0.93	0.01	24.45	131.30	0.38	0.99	0.28	0.41
4	0.002	636.63	72.46	0.41	0.17	0.005	19.47	135.28	0.37	0.93	0.26	0.39
5	0.01	24.92	122.84	0.43	0.91	0.02	27.32	123.56	0.38	0.96	0.30	0.41
6	0.008	656.80	47.95	0.41	0.88	0.003	22.58	138.78	0.37	0.83	0.26	0.39
7	0.01	28.21	123.32	0.44	0.87	0.03	32.15	121.77	0.37	0.96	0.30	0.41
8	0.005	4.66	103.45	0.52	0.81	0.01	5.38	103.14	0.39	0.84	0.44	0.47
9	0.003	0.0002	107.46	0.53	0.29	0.02	30.25	98.70	0.37	0.21	0.44	0.47

The volume of the drops studied ranges from 0.25 to 0.45 µl. The polar radius oscillates with an amplitude of 2 to 5 times higher than the equatorial radius. This could happen due to the 5:1 force ratio of the axial to the radial force of the acoustic field. The damping constant and oscillation frequency difference between the two radii are 0.5 $\frac{1}{s}$ to 30 $\frac{1}{s}$ and 0.3 Hz to 8 Hz, except for two measurements where the difference jumps significantly more than 600 $\frac{1}{s}$ and 50 Hz, respectively. This proves that the two experiments experience a running mode behaviour during the damped oscillation. One cause could the error in measurement procedures of the process. The coefficient of determination follows the same trend. Excluding the two experiments which have the coefficient of determination worse than 0.3, the coefficient of determination is better than 0.8 for the other measurements.

With results from table 4.3, interfacial tension and viscosity can be calculated using equation (eq.) (4.9) to eq. 4.12 or eq. (4.14) to eq. (4.15). The Ohnesorge number is calculated for all drops to justify the use of eq (4.9) to eq. (4.12). Interfacial tension of water in CO_2 measured with acoustic levitation is compared to Georgiadis2010 [40], Hebach2002 [41] who used pendant drop method, and Chun1995 [42] who used capillary rise method to measure interfacial of the water – carbon dioxide system.

Table 4.4: Results of interfacial tension determination using acoustic levitation

Temperature	Pressure	Interfacial Tension				
		Acoustic levitation with Oscillating drop	Literature	Method	Value	Deviation
K	MPa	mN/m	-	-	mN/m	%
298	4	6.44	Georgiadis2010	Pendant drop	47.02	86.30
			Hebach2002	Pendant drop	51.70	87.54
			Chun1995	Capillary rise	51.41	87.47
313	8	5.25	Georgiadis2010	Pendant drop	33.47	84.31
			Hebach2002	Pendant drop	47.50	88.95

The results obtained from drop shape oscillations deviates greatly by an average of 86.91 % from literature data. This argues with the results from Kremer2018, in which the average deviation of interfacial tension at all temperature with CO_2-saturated PEG400 obtained is only 20 % [2]. From this it can be inferred that the carried-out measurement of interfacial tension does not provide dependable results.

Table 4.5: Results of viscosity determination using acoustic levitation

Temperature	Pressure	Viscosity			
		Acoustic levitation with Oscillating drop	Literature	Value	Deviation
K	MPa	mPas	-	mPas	%
298	4	0.89	Nagashima 1977	6.39	86.07
313	8	0.68	Nagashima 1977	0.77	11.69

Table 4.5 compares the measured viscosity from acoustic levitation to the literature results from Nagashima 1977 [43]. The literature results are interpolated since the exact data point is not available. In average, the acoustic levitation values, correlated with the viscosity model, deviate 86.07 % for measurements at 4 MPa and 298K and 11.69% for measurements at 8 MPa and 313K from the literature data Nagashima 1977. The deviation between the literature values and the acoustic levitation data significantly decreases with increasing pressure.

Interfacial tension and viscosity measurement using acoustic levitation provides unreliable results for several causes. One reason might occur from the operating of the setup. It is possible that the acoustic levitator plant is not correctly operated. Thus, during the damped oscillation, the liquid drop might not perform a single mode oscillation in resonance frequency but exhibits a running mode. This brings about the unwanted measurement of the oblate-prolate oscillation overlapping with rotation mode. Additionally, since experiments point out that phase equilibrium might not be reached during properties measurements. This might lead to the production of the inconsistent and undependable results. Furthermore, with increase in pressure, quality of the captured images decreased. To balance this phenomenon, the high-speed camera is adjusted several times throughout the measurement process. As a result, image processing and interfacial tension and viscosity determination are unable to provide reliable results. Moreover, the size of the set of results is relatively small, lowering the accuracy and precision of the data obtained. Due to the image analysis process, only 45 % of the total recorded measurement produce results. While running the Matlab© code, the experiments that does not produce data all encounter an error in which the drop's contour cannot be determined. By comparing the measurements' images, it is deduced that the failed experiments all have significantly smaller sized drop. This could be an important note for further study of properties measurement using acoustic levitation in combination with the provided Matlab© code.

5. CONCLUSION

In this thesis, a commissioning of an acoustic levitator was conducted. The density, interfacial tension, and viscosity of liquids inside a saturated CO2 environment are evaluated using acoustic levitation. The underlying concept as well as the state of the art in acoustic levitation measurements are discussed in this thesis so that the setup and its purpose can be understood. Then, the configuration of the high-pressure acoustic levitator plant and functions of the components are discussed completely. Furthermore, the measuring procedures are put to the test under extreme conditions. While density determination is done under ambient condition, interfacial tension and viscosity determination are done in 4 MPa at 298 K and 8 MPa at 313 K. Finally, the findings are compared to data from the literature. Then, the constraints and restrictions of the plant are discussed. For density measurement under ambient pressure, the obtained results are in agreement with literature data, proving that acoustic levitation is a reliable method. However, due to the unreproducible drop volume and transducer-reflector position for repeating measurement, it is impossible to measure density under high pressure using the current setup. For interfacial tension and viscosity determination under pressure, the measured data deviates significantly from literature value and therefore is concluded to be unreliable. This could be the consequence of error in operations of the plant or limitation of the plant itself. First, experiments point out that the system might not reached phase equilibrium during measurement, leads to an inconsistent result. Next, due to operation error, there might be an overlap of oblate-prolate oscillation and rotation modes. This results in incorrect calculation for interfacial tension and viscosity. During the measurement, the high-speed camera zoom must be adjusted multiple times to avoid capturing the blurry images cause by increasing pressure. Also, the size of the set of the results is small, results in unreliable data. This is cause by the long time needed to set up the plant and the Matlab© only process half of the taken images. Moreover, due to the misaligned reflector cause by removing the capillary from the sound field, the drop might fall out of the focus of the high-speed camera. This might cause some problems to the image analysis process. All in all, it is clear that acoustic levitation provides a great method of investigating liquid droplets without wall-contacting. However, due to its limitations, the results obtained is unreliable. Therefore, it is crucial to assess these limitations and provide solutions to improve the current setup.

REFERENCES

References

1. Boroša DJ (2013) Entwicklung und Aufbau eines akustischen Levitators zur Untersuchung von Stofftransport- und Partikelbildungsmechanismen von Proben unter hohen Drücken
2. Kremer J (2018) On the measurement of physical properties in high pressure systems using acoustic levitation
3. Morris RH, Dye ER, Docker P et al. (2019) Beyond the Langevin horn: Transducer arrays for the acoustic levitation of liquid drops. Physics of Fluids 31:101301. https://doi.org/10.1063/1.5117335
4. Simon MD, Geim AK (2000) Diamagnetic levitation: Flying frogs and floating magnets (invited). Journal of Applied Physics 87:6200–6204. https://doi.org/10.1063/1.372654
5. Rhim W-K, Chung SK (1991) Containerless protein crystal growth method. Journal of Crystal Growth 110:293–301. https://doi.org/10.1016/0022-0248(91)90898-F
6. Ashkin A, Dziedzic JM (1971) Optical Levitation by Radiation Pressure. Appl Phys Lett 19:283–285. https://doi.org/10.1063/1.1653919
7. Winborne DA, Nordine PC, Rosner DE et al. (1976) Aerodynamic levitation technique for containerless high temperature studies on liquid and solid samples. MTB 7:711–713. https://doi.org/10.1007/BF02698607
8. T. G. Wang (1979) Acoustic levitation and manipulation for space applications,
9. Marco A. B. Andrade, Asier Marzo, and Julio C. Adamowski (2020) Acoustic levitation in mid-air: Recent advances, challenges, and future perspectives. Appl. Phys. Lett 116
10. Marco A. B. Andrade, Nicolás Pérez, and Julio C. Adamowski (2017) Review of Progress in Acoustic Levitation
11. E. G. Lierke (1996) Akustische Positionierung – Ein um-fassender Überblick über Grundlagen und Anwendungen. Acustica 82:220–237
12. A. L. Yarin, M. Pfaffenlehner, C. Tropea (1998) On the acoustic levitation of droplets. J. Fluid Mech. 356:65–91
13. R. Tuckermann (2002) Gase, Aerosole, Tropfen und Partikel in stehenden Ultraschallfeldern: Eine Untersuchung zur Anreicherung schwerer Gase, Verdampfung levitierter Tropfen, Kristall- und Partikelbildung
14. R. Tuckermann, S. Bauerecker, B. Neidhart (2001) Levitation in Ultraschallfeldern - Schwebende Tröpfchen 2:69–75
15. Doerr FJ, Oswald ID, Florence AJ (2018) Quantitative investigation of particle formation of a model pharmaceutical formulation using single droplet evaporation experiments and X-ray tomography. Advanced Powder Technology 29:2996–3006. https://doi.org/10.1016/j.apt.2018.09.027
16. Sloth J, Kiil S, Jensen AD et al. (2006) Model based analysis of the drying of a single solution droplet in an ultrasonic levitator. Chemical Engineering Science 61:2701–2709. https://doi.org/10.1016/j.ces.2005.11.051

17. Cerenius Y, Oskarsson Å, Santesson S et al. (2003) Preliminary tests on the use of an acoustic levitator for liquid X-ray diffraction experiments. J Appl Crystallogr 36:163–164. https://doi.org/10.1107/S0021889802019209
18. Leiterer J, Delissen F, Emmerling F et al. (2008) Structure analysis using acoustically levitated droplets. Anal Bioanal Chem 391:1221–1228. https://doi.org/10.1007/s00216-008-2011-2
19. Leiterer J, Emmerling F, Panne U et al. (2008) Tracing coffee tabletop traces. Langmuir 24:7970–7978. https://doi.org/10.1021/la800768v
20. Tsujino S, Tomizaki T (2016) Ultrasonic acoustic levitation for fast frame rate X-ray protein crystallography at room temperature. Sci Rep 6:25558. https://doi.org/10.1038/srep25558
21. Leiterer J, Leitenberger W, Emmerling F et al. (2006) The use of an acoustic levitator to follow crystallization in small droplets by energy-dispersive X-ray diffraction. J Appl Crystallogr 39:771–773. https://doi.org/10.1107/S0021889806024915
22. Delissen F, Leiterer J, Bienert R et al. (2008) Agglomeration of proteins in acoustically levitated droplets. Anal Bioanal Chem 392:161–165. https://doi.org/10.1007/s00216-008-2252-0
23. Radnik J, Bentrup U, Leiterer J et al. (2011) Levitated Droplets as Model System for Spray Drying of Complex Oxides: A Simultaneous in Situ X-ray Diffraction/Raman Study. Chem Mater 23:5425–5431. https://doi.org/10.1021/cm202674f
24. Leopold N, Haberkorn M, Laurell T et al. (2003) On-line monitoring of airborne chemistry in levitated nanodroplets: in situ synthesis and application of SERS-active Ag-Sols for trace analysis by FT-Raman spectroscopy. Anal Chem 75:2166–2171. https://doi.org/10.1021/ac026308l
25. Wood BR, Heraud P, Stojkovic S et al. (2005) A portable Raman acoustic levitation spectroscopic system for the identification and environmental monitoring of algal cells. Anal Chem 77:4955–4961. https://doi.org/10.1021/ac050281z
26. S. Biedasek, M. Abboud, H. U. Moritz, and A. Stammer (2007) Online-analysis on acoustically levitated droplets 259:390–396
27. Lee S, Ohsaka K, Rednikov A et al. (2006) Noncontact thermophysical property measurement by levitation of a thin liquid disk. Annals of the New York Academy of Sciences 1077:75–95. https://doi.org/10.1196/annals.1362.060
28. Sebastian Baer, Cemal Esen and Andreas Ostendorf (2014) Phase equilibrium measurements of acoustically levitated squalane–CO2 mixtures by Raman spectroscopy
29. Borosa D, Brinkmann J, Kareth S et al. (2014) Vergleich des Stofftransports von hängenden und akustisch levitierten Wassertropfen in CO 2. Chemie Ingenieur Technik 86:666–674. https://doi.org/10.1002/cite.201300150
30. M. Achatz, W. Heide, E. G. Lierke, G. H. Seger (1978) Verfahren und Vorrichtung zur Bestimmung von Dichte, Oberflächenspannung und Viskosität an kleinen Flüssig-keitsvolumina,
31. R. E. Apfel, R. G. Holt, Y. Tian, T. Shi, X. Zheng (1993) Surface characterization through shape oscillations of drops in microgravity and 1-g.:339

32. Trinh EH, Ohsaka K (1995) Measurement of density, sound velocity, surface tension, and viscosity of freely suspended supercooled liquids. Int J Thermophys 16:545–555. https://doi.org/10.1007/BF01441920
33. P. L. Marston (1980) Shape oscillation and static deformation of drops and bubbles driven by modulated radiation stresses 67 (1):15
34. C.-J. Hsu, R. E. Apfel (1987) Model for the quadrupole oscillation of drops for determining interfacial tension 82 (6):2135
35. G. J. Lauth, J. Kowalczyk (2016) Einführung in die Physik und Chemie der Grenzflächen und Kolloide
36. P. Atkins, J. de Paula (2014) Atkins' physical chemistry
37. R. B. Bird, W. E. Stewart, E. N. Lightfoot (2002) Transport phenomena
38. G. Schramm (2002) Einführung in die Rheologie
39. H. Schlichting KG (2006) Grenzschicht-Theorie
40. Georgiadis A, Maitland G, Trusler JPM et al. (2010) Interfacial Tension Measurements of the (H 2 O + CO 2) System at Elevated Pressures and Temperatures. J Chem Eng Data 55:4168–4175. https://doi.org/10.1021/je100198g
41. Hebach A, Oberhof A, Dahmen N et al. (2002) Interfacial Tension at Elevated PressuresMeasurements and Correlations in the Water + Carbon Dioxide System. J Chem Eng Data 47:1540–1546. https://doi.org/10.1021/je025569p
42. Byung-Soo Chun/Gordon T. Wilkinson (1995) Interfacial tension in high-pressure carbon dioxide mixtures. Ind. Eng. Chem. Res. 34:4371–4377
43. Nagashima A (1977) Viscosity of water substance—new international formulation and its background. Journal of Physical and Chemical Reference Data 6:1133–1166. https://doi.org/10.1063/1.555562
44. Lord Rayleigh (1879) On the capillary phenomena of jets:71
45. H. Lamb (1932) Hydrodynamics 6th edition:475
46. E. Becker, W. J. Hiller, T. A. Kowalewski (1991) Experimental and theoretical investigation of large amplitude oscillations of liquid droplets 231:189
47. P. L. Marston, R. E. Apfe (1980) Quadrupole resonance of drops driven by modulated acoustic radiation pressure – Experimental properties 67:27
48. J. Kremer, A. Kilzer, M. Petermann (2018) Simultaneous measurement of surface tension and viscosity using freely decaying oscillations of acoustically levitated droplets 89 (1)
49. Faria MAF, Martins RJ, Cardoso MJEM et al. (2013) Density and Viscosity of the Binary Systems Ethanol + Butan-1-ol, + Pentan-1-ol, + Heptan-1-ol, + Octan-1-ol, Nonan-1-ol, + Decan-1-ol at 0.1 MPa and Temperatures from 283.15 K to 313.15 K. J Chem Eng Data 58:3405–3419. https://doi.org/10.1021/je400630f

APPENDIX

Table A: Measurement data under ambient pressure: Density

No.	Drop-out		
	Water	Ethanol	Waterglass
	Vpp	Vpp	
E_211210_1	9.4	8.5	10.1
E_211210_2	8.2	9.8	10.6
E_211210_3	8.7	9.6	9.5
E_211210_4	9.5	7.2	8.4
E_211210_5	9.4	8.1	10.7
E_211210_6	10.8	7.1	10.2
E_211210_7	10.7	8.8	9.7
E_211210_8	10.9	8.5	9.6
E_211210_9	9.8	8.6	9.4
E_211210_10	9.6	8.5	8.8

Table B: Measurement data under high pressure: shape oscillations

Name	System	Temperature	Pressure	Carrier signal		Amplitude modulation	
				Frequency	Amplitude	Frequency	Depth
		°C	bar	Hz	Vpp	Hz	%
E_211215_1	Distilled water-CO2	24.6	41.7	31805	17.5	100	10
E_211215_2		24.6	41.7	31805	17.5	100	10
E_211215_3		24.7	41.8	31805	17.5	100	10
E_211215_4		24.7	41.6	31805	17.5	100	10
E_211215_5		24.7	41.6	31805	17.5	100	10
E_211215_6		25.1	41	31805	17.5	100	10
E_211215_7		25.1	41	31805	17.5	100	10
E_211215_8		25.1	41	31805	17.5	100	10
E_211215_9		25.2	42.5	31805	17.5	100	10
E_211215_10		25.1	42.5	31805	17.5	100	10
E_211215_11	Distilled water-CO2	24.6	41.6	31805	17.5	100	10
E_211215_12		24.8	41.7	31805	17.5	100	10
E_211215_13		25.1	41	31805	17.5	100	10
E_211215_14		25.1	41	31805	17.5	100	10
E_211215_15		24.6	41.7	31805	17.5	100	10
E_211215_16		24.6	41.7	31805	17.5	100	10
E_211215_17		24.6	41.7	31805	17.5	100	10
E_211215_18		24.6	41.7	31805	17.5	100	10
E_211215_19		24.6	41.7	31805	17.5	100	10
E_211215_20		24.6	41.7	31805	17.5	100	10
E_211217_1	Distilled water-CO2	40.3	79.9	32128	17.5	50	10
E_211217_2		40.3	79.2	32128	17.5	55	10
E_211217_3		39.5	78.6	32128	17.5	55	10
E_211217_4		41.7	81.3	32128	17.5	55	10
E_211217_5		39.5	80.8	32128	17.5	55	10
E_211217_6		40.5	81.4	32128	17.5	55	10
E_211217_7		39.3	80.5	32128	17.5	45	10
E_211217_8		40.7	80.3	32128	17.5	43	10
E_211217_9		40.7	80.3	32128	17.5	43	10
E_211217_10		40.7	80.3	32128	17.5	43	10
E_211217_11	Distilled water-CO2	39.4	79.3	32128	17.5	50	10
E_211217_12		40.1	79.1	32128	17.5	55	10
E_211217_13		39.5	78.6	32128	17.5	55	10
E_211217_14		39.7	80.7	32128	17.5	55	10
E_211217_15		40.1	81.3	32128	17.5	55	10
E_211217_16		40.1	81	32128	17.5	55	10
E_211217_17		39.5	80.8	32128	17.5	45	10
E_211217_18		39.6	80.6	32128	17.5	43	10
E_211217_19		40.7	80.3	32128	17.5	43	10
E_211217_20		40.7	80.3	32128	17.5	43	10

DECLARATION OF ORIGINALITY

I confirm, that the submitted thesis is original work and has been written by me without further assistance. Appropriate credit has been given where reference has been made to the work of others. Moreover, I confirm, that the thesis was not examined before, nor has been published.

_____ _____

Datum Unterschrift